Reducing Radiation Dose for a Linear Slot Scanning Digital X-ray Machine using a Filtration Technique

by

Timothy David Perks

SUBMITTED TO THE UNIVERSITY OF CAPE TOWN

In partial fulfilment of the requirements for the degree

MSc (Med) in Biomedical Engineering

UNIVERSITY OF CAPE TOWN
IYUNIVESITHI YASEKAPA • UNIVERSITEIT VAN KAAPSTAD

Declaration

I, Timothy David Perks, hereby declare that the work which is presented in this dissertation is my original work, except where acknowledgements indicate otherwise. Neither the whole work, nor any part of it, has been or is being submitted to another degree at this or any other university.

I give permission to the University of Cape Town and to Lodox Systems Pty (Ltd) to make use of the research content described in this dissertation either in full, or in part, for the purpose of further research.

Signed: _____ Date: _____

Abstract

This study describes the development of a filtration technique applied to the Lodox Statscan linear slot-scanning digital X-ray system to reduce radiation dose to paediatric patients whilst preserving diagnostic image quality.

The Statscan is an FDA approved, commercially available digital X-ray system commonly used for trauma and emergency patients. The Statscan provides significantly lower radiation dose to patients than conventional X-ray systems for comparable studies without loss of image quality. This is particularly beneficial in paediatric radiology, where the risks associated with ionizing radiation are much higher.

A static dose prediction model for the Statscan which was previously developed at the University of Cape Town has been adapted to create a dynamic dose prediction model which allows the user to adjust the system scanning parameters. The model calculates the patient entrance dose from an energy spectrum generated using the input parameters. The effective dose for a paediatric sized patient is then calculated using a Monte Carlo simulation. The dynamic model allows for variation of the scan parameters and direct observation of the expected dose levels for specific examinations.

Filtration is a well-known technique for reducing radiation dose, where a filter material is placed in the path of the X-ray beam to reduce patient exposure to radiation. The dynamic model was used to design a new filtration technique for the paediatric settings on the Statscan. An added filter of 1.8mm aluminium was predicted to lower the radiation dose significantly. The PTW Normi 4FLU test phantom was used for quantitative assessment, showing that image contrast and spatial resolution were maintained with the proposed filter. Ethics approval was obtained for a paediatric cadaver imaging trail, which assessed the diagnostic quality of the images and measured the dose reduction following the application of a 1.8mm aluminium filter. A panel of experienced radiologists assessed the images and found that diagnostic quality was maintained with the added filtration.

A new filtration technique for paediatric scanning on the Lodox Statscan has been developed and validated. The 1.8mm aluminium added filtration was found to reduce entrance dose for paediatric patients by 36% on average and to reduce effective dose by 27% on average, while maintaining image quality.

Acknowledgements

Dr Tania Douglas, Medical Imaging Research Unit and Biomedical Engineering Programme, University of Cape Town

Mr Stef Steiner, Lodox Systems and Medical Imaging Research Unit, University of Cape Town

Mr Christoph Trauernicht, Division of Medical Physics, Groote Schuur Hospital

Dr Benjamin Irving, University of Cape Town MSc in Biomedical Engineering graduate

Dr Linda Liebenberg, University of Cape Town and Salt River Forensic Pathology Laboratory

Ms Shirees Benjamin, Radiographer, Salt River Forensic Pathology Laboratory

Ms Nafeesah Karriem-Soeker, Radiographer, Lodox Systems

Dr Andrew Lawson, Radiologist, Red Cross Memorial Children's Hospital

Dr Tharbit Hartley, Radiologist, Groote Schuur Hospital

Dr Paul Scholtz, Radiologist, Groote Schuur Hospital

The Lodox Programme for financial assistance, resources and practical work experience

The National Research Foundation for financial assistance

My parents for their financial support and never-ending encouragement throughout my studies

My wife, Carolyn, for marrying a student and for her patience, understanding and support

Fellow Biomedical Engineering students in the Faculty, for stimulating discussions and fun along the way, specifically Jeremy Pitman, Shaun Fickling and Kieran Duggan

"Here's to you Mrs Robinson."

Contents

List of Figures

List of Tables

Glossary

Absorbed Dose in Air - D_A

The energy transferred from ionising radiation to air per unit mass of air

Anode

Current flows into the anode of a device; in the X-ray tube the electrons travel from the cathode to the anode

Antero-posterior Projection - AP

A projection with the X-ray beam passing from the front of the patient to the back

Automatic Technique Factor Correction - ATFC

Modification of the technique factors as a slit scan progresses in order to optimise the beam for the anatomy of each region of the body

Cathode

Current flows out of the cathode of a device; in the X-ray tube electrons travel from the cathode to the anode

Coulomb - C

SI derived unit of charge

Detective Quantum Efficiency - DQE

A quantifiable measure of detector performance

Dose-area Product - DAP

Entrance surface dose multiplied by the cross sectional area exposed by the beam

Effective Dose - E

Radiation dose quantity, the tissue-weighted sum of the equivalent doses in all specified tissues and organs of the body

Effective DQE

A measure of overall imaging system performance

Electron Volt - eV

Unit of energy where $1eV = 1.602 \times 10^{19}$ J

Entrance Dose “free-in-air"

Dose in air at the patient surface excluding backscatter

Entrance Surface Dose - ESD

Dose in air at the patient surface including backscatter

Exposure - X

Amount of charge per unit mass produced by ionising radiation in air

Filtration

The technique of placing a filter material into the path of an X-ray beam to remove unnecessary photons before the beam interacts with the target object

Focus-to-collimator Distance - FCD

The distance from the X-ray focal spot to the collimator

Focus-to-skin Distance - FSD

The distance from the X-ray focal spot to the surface of the patient

Gray - Gy

Unit of dose where 1 Gy= 1 J/kg

Grey Scale

A scale used in the assessment of colour contrast within an image

Hertz - Hz

SI derived unit of frequency.

International Committee for Radiological Protection - ICRP

An international advisory body on radiation protection

Ionisation Chamber

A chamber used to measure exposure and dose

Ionising Radiation

Electromagnetic radiation with enough energy to ionise atoms

Joules - J

SI derived unit of energy

Lateral Projection - LAT

A projection where the X-ray beam passes through the side of the patient

Monte Carlo Simulations

Used in medical physics applications to simulate the path of electrons, photons or other particles through the body during treatment or diagnostics; used to estimate risk

PCXMC

A commercially available Monte Carlo simulator which can be used to simulate X-ray examination scenarios theoretically

Photon

A quantum/particle of electromagnetic radiation

Roentgen - R

Unit of exposure where 1R = 2.58 x 10^{-4} C/ kg

Sievert - Sv

Unit of effective dose and equivalent dose where 1 Sv =1 J/kg

Statscan

A commercially available linear slot scanning digital X-ray machine

Technique Factors

Parameters that can be changed to optimise the X-ray image quality

Tube Current - mA

The current from to the flow of electrons from the cathode to the anode of the X-ray tube, typically measured in mA

Tube Voltage - kV

The potential difference between the cathode and the anode of the X-ray tube, typically measured in kV

Volt - V

SI derived unit of electric potential

X-ray Spectrum

A graphical depiction of the flux of photons against the kV range of the X-ray beam

X-rays

High energy electromagnetic radiation derived from interactions outside the atomic nucleus

1. Introduction

X-ray imaging, and more recently digital X-ray imaging, is a common practice in medical facilities around the world to review internal anatomy in the human body. Since the earliest discovery of X-rays by Wilhelm Roentgen, the harmful effect of ionizing radiation has been well documented, especially with regard to children. The risks associated with paediatric radiology in the form of ionizing radiation are higher than in adults (Ron 2011; Brosi et al. 2011). Medical imaging with X-ray technology strives to provide the reviewing radiologist with an image that has quality appropriate to the task of diagnosis, whilst providing the minimum dose to the patient (Martin et al. 1999).

The harmful effects of radiation can be lessened through the use of various filtration techniques which alter the energy in the X-ray beam. Several studies have shown that increased filtration of the X-ray beam spectrum to the patient reduces radiation, both in children and in adults (Hansson et al. 1997). A disadvantage of filtration of the X-ray beam is that it is known to diminish image contrast, although modern post-processing techniques have enabled partial recovery of this lost contrast (Hamer et al. 2005).

This project examined the application of filtration to the Lodox Statscan digital X-ray scanner, with the aim of reducing dose whilst maintaining diagnostic image quality.

1.1 Lodox Statscan

The Lodox Statscan, shown in Figure 1, is a linear slot scanning radiography (LSSR) system which has been approved by the FDA and is commercially available. It is commonly used for trauma and emergency patients (Evangelopoulos et al. 2010).

The Statscan uses a C-Arm system traversing the patient trolley at a selected scanning speed, which ranges between 35 and 140 mm/s. A full body scan can be completed in 13 seconds. The X-ray beam produced by at the source is collimated into a fan-beam (0.4mm or 1mm in width), which passes through the patient to the detector. The detector makes use of a bank of charge-coupled-device cameras. The captured images are immediately available at the workstation monitor following the completion of the scan. The C-arm of the Statscan can rotate axially over the bed to provide the possibility of anteroposterior, oblique and lateral examinations, up to a maximum angle of 100°. The linear slot-scanning technique produces a two-dimensional diagnostic-quality image at a reduced patient exposure level when compared to conventional X-ray systems (Szucs-Farkas & Vock 2009).

Figure 1: Lodox Statscan full body digital X-ray imaging system

The Statscan has been used successfully in several paediatrics applications (Douglas et al. 2008). A three-year study with a Lodox Statscan dedicated to paediatric radiology found that the scanner produces diagnostic quality X-rays with significantly lower radiation levels than conventional radiography (Douglas et al. 2008).

1.2 Objectives

This research project aimed to find a new suitable filtration technique to lower the amount of ionizing radiation dose to which paediatric patients are exposed when scanned using the Lodox Statscan.

Specifically, the objectives were to:

- Validate an existing 0.1mm Cu filter used for large adult studies on the Lodox Statscan, in order to test the claim of dose reduction while maintaining image quality in current practice.
- Develop a dynamic dose prediction model, in order to explore an extension of the current filtration practice for large adults to paediatric imaging.
- Use the dose prediction model to design a filtration technique for paediatric imaging.
- Validate the paediatric filtration technique in a phantom study and a clinical study.

1.3 Dissertation Outline

The dissertation begins with a literature review (Chapter 2) covering the topics of radiography, dose prediction, dose measurement, filtration and image quality assessment.

Chapter 3 validates an existing 0.1mm Cu filter used for large adult studies on the Lodox Statscan, in order to test the claim of dose reduction while maintaining image quality in current practice.

Chapter 4 describes the modification of a static dose prediction model to create a dynamic dose prediction model, in order to extend the current practice for large adults, as validated in Chapter 3, to paediatric imaging. The model is used to propose a filter for paediatrics.

Chapter 5 examines the effects of filtration at paediatric settings on dose and image quality in a non-clinical environment, using phantoms, and proposes a new paediatric filtration technique.

Chapter 6 applies the new paediatric filtration technique to paediatric cadavers.

Chapter 7 concludes the dissertation.

1.4 Dissertation contribution

The dissertation makes the following contributions to medical science:

- The current 0.1mm copper filtration technique applied to the Lodox Statscan for high kV studies has been validated to significantly reduce dose whilst maintaining image quality.
- A previously developed dose prediction model has been adapted and may be used to test the effect of filter materials at different scanning parameters.
- A new filtration technique for paediatric scanning on the Lodox Statscan has been developed and validated, which reduces paediatric dose while maintaining image quality.

A paper was presented at an international conference: T.D. Perks, C. Trauernicht ,T. Hartley, C. Hobson, A. Lawson, P. Scholtz, R. Dendere, S. Steiner, and T.S. Douglas. “Effect of Aluminium Filtration on Dose and Image Quality in Paediatric Slot-Scanning Radiography.” *35th Annual International IEEE EMBS Conference Osaka*, July 2013.

2. Literature Review

This chapter reviews the following to provide a basis for the development of a filtration technique for paediatric X-ray imaging: digital and paediatric radiology, dose prediction, filtration in X-ray imaging and image quality evaluation.

X-rays were first discovered by Wilhelm Roentgen in 1895. During the first few decades in which X-ray technology was developed and improved, there was a severe lack of understanding regarding the dangers of ionizing radiation to the human body. Some examples of the ignorance include public demonstrations of X-rays being produced in some department stores, proposals for X-rays to be used in pregnancy diagnostics, and even the use of X-rays to remove unwanted hair (Walker 2000).

In the early years of X-ray experimentation, some cases of skin rashes and sore eyes were noted from prolonged exposure to the radiation. In 1904, Clarence Dalley, Thomas Edison's laboratory assistant, died a painful death after acute exposure to X-rays. Within two years of the discovery of X-rays, it was understood that it had harmful consequences. In the early 1900's, simple methods of shielding were recommended for X-ray operators. But it wasn't until 1921, after World War I where medical X-ray technology was widely used and misused, that a radiation protection committee was tasked with drawing up a set of recommendations for safe X-ray examinations (Walker 2000).

The carcinogenic effect of ionising radiation has been the subject of much investigation since the first effects were noted, and much research emphasis has been placed on measuring the amount of radiation to which a patient is exposed – and the effect of this radiation in causing different cancers (Ron 2011).

In 1934, a "tolerance dose" was recommended by the International Commission of Radiation Protection (ICRP) to set a limit for daily exposure to radiation. After the end of World War II and the advent of atomic bombs, public health views and increased awareness of the dangers of radiation exposure, combined with experimental research, prompted the creation of much lower "maximum permissible dose" to replace previous tolerance levels. This was a result of the research showing that even low levels of exposure to radiation had harmful effects (Regano & Sutton 1992).

Even with decades of research, the ionizing radiation produced by X-ray generation continues to be a health risk in medical imaging.

2.1 Digital Radiography

For over a century, radiography using film to capture the image has been standard practice. Reducing radiation dose to the patient was at first not as important as obtaining an adequate image, and many hospitals were overcompensating with dose in order to obtain a better quality image. In recent times more emphasis has been placed on optimising imaging conditions to obtain better images while attempting to lower dose (Martin 2007).

The advent of digital imaging has revolutionised the medical imaging field. Digital technology allows for flexibility within diagnostic imaging, where adequate images can be obtained at much lower radiation levels (Martin et al. 1999). Digital detectors have been found to produce images equal or superior to those of conventional screen-film systems. The benefit of the large dynamic range available with digital radiography systems, is that there are many possibilities for optimising the patient dose and image quality ratio, although evaluating the dose reducing effects is a much easier task compared to evaluating the effects on image quality (Smet 2012).

The expanding range of digital imaging systems leads to a new challenge to radiology: medical physicists and radiologists need to collaborate and find which form of digital radiography is most effective for a particular study, and whether the performance of the system meets the expectations (Dobbins 2000).

These advantages have led to digital systems becoming the current gold standard in radiography (Smet 2012).

2.2 Paediatric Radiology

The risks associated with paediatric radiology in the form of ionizing radiation are higher than in adult radiology (Ron 2011). While children are growing, their cells are rapidly dividing, which makes them prone to increased DNA damage from radiation. These effects may predispose to malignant changes in later life, as the sum of damage to biological tissue from radiation increases over a lifetime (Evangelopoulos et al. 2010; Gislason et al. 2010). The lifetime risk for fatal cancer related to dose exposure is 14% per Sv for children aged between 0 and 9 years, compared to a much lower 4% per Sv for adults at an age of 30 years (Hansson et al. 1997). For these reasons, radiation dose must be kept to an absolute minimum for paediatric patients, provided suitable image quality is maintained (Hansson et al. 1997; Evangelopoulos et al. 2010; Gislason et al. 2010).

2.3 Radiation Exposure

Radiation protection principles require the radiation dose to a patient to be as low as is reasonably possible with the medical purposes of the examination being accomplished (Smans et al. 2010), (Mooney & Thomas 1998), (Francke et al. 2001). Image quality is the major trade off when lowering radiation, and diagnostic image quality must be maintained while lowering dose to a minimum (Slovis 2002).

An X-ray is a form of electromagnetic radiation that is energetic enough to liberate electrons from atoms which fall into its path. This effect an X-ray has on matter is measured using an ionization chamber, which is an air-filled chamber enclosed between positive and negative electrodes. The molecules of air present in the chamber are ionized when the chamber falls in the path of an X-ray beam, and the net charge is collected at the electrodes (Beutel et al. 2000).

Traditionally, exposure is measured in Roentgen, where:

$$1R = 2.58 \times 10^{-4}\ C/kg$$

where the typical ionization chamber has a mass of approximately 7.8mg of air, and thus one Roentgen of ionized exposure to that air will realise a charge of 2.0×10^{-9} C.

While the Roentgen (R) is the traditional unit of exposure, the Gray (Gy) is the SI unit for the dose absorbed by air, where:

$$\text{Entrance Dose (Gy)} = 0.00876(R)$$

In modern medical physics, there are two main categories into which dose can be separated: entrance surface dose and effective dose.

2.3.1 Entrance Surface Dose

Entrance dose (free in air) refers to the amount of energy transferred from ionising radiation to the air per unit volume, due to the interactions between the X-ray beam and the atoms in the air. This free in air dose does not take into account the effects of backscatter.

Entrance surface dose, sometimes referred to as entrance skin dose, is the measure of radiation at the point where the X-ray beam makes contact with the patient. This measure does not take into account the effect of radiation on different organs and tissues, although it does it account for backscatter (Gogos et al. 2003). Entrance surface dose is used as the standard for setting dose levels for common radiographic examinations in adults, and children (Mooney & Thomas 1998).

The unit for entrance surface dose measurement is Gray (Gy), where:

$$1Gy = 1\ J/Kg$$

Unless otherwise stated, “dose” in this document refers to entrance surface dose.

2.3.2 Effective Dose

Effective dose (E) is defined by the International Commission on Radiological Protection (ICRP) as the weighted average of the equivalent dose to each organ in the body. In other words, E the measure of the amount of radiation to which a whole body is exposed, taking into account the fact the ionizing radiation is distributed in a non-uniform manner to different parts of the body.

The unit for effective dose is the Sievert (Sv), where:

$$1Sv = 1\ J/Kg$$

1mSv per year is the maximum recommended exposure for the general public (ICRP 2007).

2.4 Dose Prediction

The risks associated with ionising radiation are often not fully understood by radiologists, which can often lead to patients being exposed to higher levels of radiation than what is necessary for their radiographic procedure (Slovis 2002).

Entrance dose can be theoretically calculated from the energy spectrum of an X-ray beam. An accurate method has been developed and validated for generating tungsten anode X-ray spectra from 30 to 140 kV (Boone & Seibert 1997). This method has been successfully used previously to model the entrance dose for linear slot-scanning radiography (LSSR) (Scheelke et al. 2005).

Effective dose calculations differ from those of entrance dose, in that the effective dose takes into account the characteristics of the beam, the patient size and shape as well as the type of examination being performed (Irving 2008). Effective dose is calculated as the sum of the product of the absorbed dose of the organs and the appropriate weighting factors of the organs. The organs’ absorbed dose may be determined from the entrance dose.

The majority of work on dose prediction modelling has been directed towards conventional full field radiography units. These methods make use of Monte Carlo simulators to calculate the effective dose.

2.4.1 Monte Carlo Simulators

A Monte Carlo simulator is a computerised mathematical technique used in medical physics applications, which simulates the path of electrons, photons or other particles through the body. These applications allow the user to simulate a variety of scenarios to assess how a particular model would behave under certain input variables. These simulators allow the ability to assess scenarios which would be difficult, or in some cases impossible, to measure physically (Boone 1992). Monte Carlo simulator have commonly been used to calculate the effective dose to patient from X-ray exposure during imaging (Hamer et al. 2005; Brosi et al. 2011; Martin et al. 1999; Evangelopoulos et al. 2010; Irving et al. 2008).

PCXMC is a commercially available Monte Carlo application has been used in several studies related to effective dose for LSSR (Exadaktylos et al. 2008; Evangelopoulos et al. 2010; Trauernicht et al. 2012; Irving et al. 2008). PCXMC uses Monte Carlo simulations to predict the path of photons emitted from the beam source, taking into account any added filtration, the examination technique factors, the patient dimensions and the photon interactions with each organ. The simulator uses a mathematical phantom to calculate the cross section of tissue affected by the incident photons The effective dose is then calculated from the amount of energy which is absorbed by each organ (Irving 2008). PCXMC does not calculate effective dose strictly according to the ICRP103 specifications (Tapiovaara & Siiskonen, 2008): “the effective dose is calculated using size-adjustable hermaphrodite phantoms, whereas the present ICRP (2007) definition specifies that the organ doses are calculated in a reference male phantom and in a reference female phantom, the equivalent organ doses in these two phantoms are averaged, and the effective dose is obtained as a weighted sum of these sex-averaged organ doses.”

2.4.2 Dose prediction for linear slot scanning radiography

The major difference between linear slot scanning (LSSR) and conventional scanning is that the conventional method captures the entire image at once from a stationary source, while with LSSR the source of the beam moves linearly across the patient capturing the image slice by slice. In the diagram below (Figure 2), the figure on the left displays a conventional stationary source providing a uniform field of radiation to capture an image. The figure on the right depicts a moving source common in LSSR, where a narrow fan beam from the C-arm moves along the length of the table scanning the patient. The CCD cameras continuously collect the image data as the patient is scanned. The narrow and vertical fan beam scans linearly over the patient, and at the detector distance the beam is 3-6mm in width and 700mm in length (size of detector CCD bank), while the beam shape is set by the collimator slot which is described below. A second collimator at the detector is used to remove any scattered radiation that is not part of the desired beam area. The narrow beam and detector combination dramatically reduces the amount of backscatter when compared to conventional radiography, and this is the primary reason why LSSR provides a significantly lower dose to patients when compared to conventional radiography (Scheelke et al. 2005).

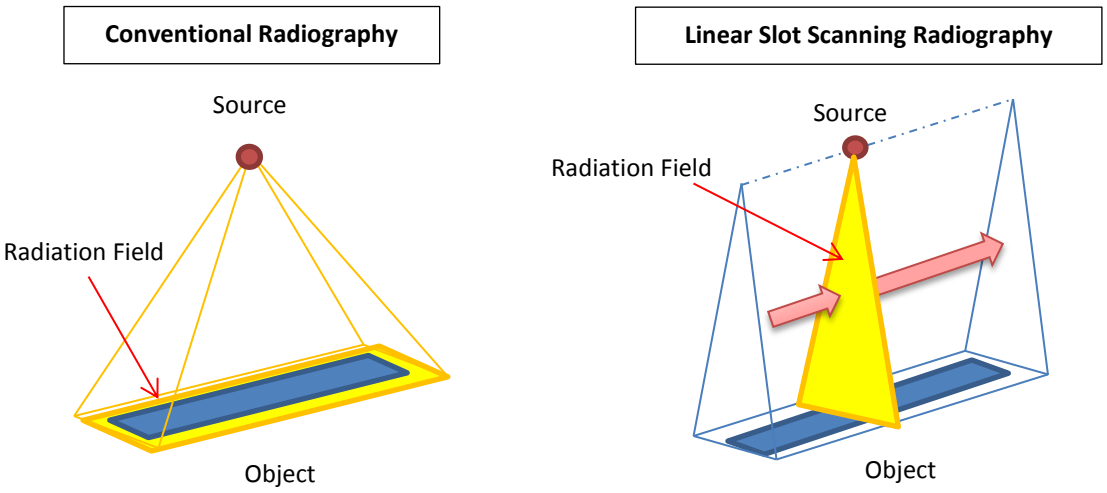

Figure 2: Conventional single point source X-ray beam (left) and LSSR X-ray beam moving over the object (right).

The fan beam described above is created by focussing the source beam through a slot between two solid metal plates. These plates make up the collimator, which limits the field of the X-ray beam. For the Lodox Statscan, the collimator is adjustable depending on the scanning technique factors needed, allowing collimator widths of 0.4mm or 1mm. The collimator width has a direct effect on the amount of photons to which a patient is exposed, and this factor, along with the tube current and the scanning speed, is linearly related to the entrance dose and effective dose a patient receives (Irving et al. 2008)

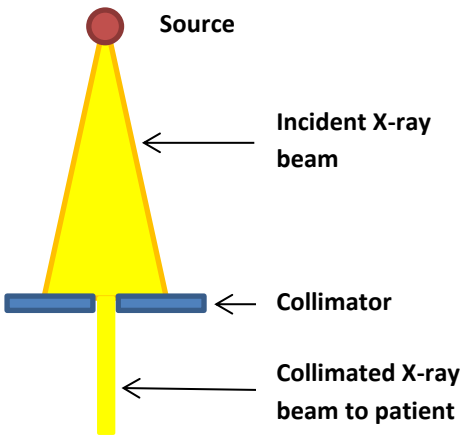

Figure 3: Collimation of incident X-ray beam to become a fan beam.

A dose prediction model for LSSR was developed and verified at the University of Cape Town in 2008. The model successfully predicted entrance dose and effective dose for the Statscan (Irving 2008). The method is described below.

The model uses a spectrum generation model to calculate the expected entrance dose. The spectrum generation model is a method successfully used by (Boone & Seibert 1997) to predict entrance dose. The method calculates the energy of the beam in terms of photon flux per unit mAs.

For LSSR, the effective mAs is calculated linearly but multiplying the tube current by the exposure time:

$$mAs = mA\frac{Focus\ to\ Skin\ Distance}{Focus\ to\ Collimator\ Distance}x\frac{collimator\ width}{scan\ speed}$$

This can be used to calculate the mAs at any given point during the scan. With the mAs and the input tube voltage, the next step in the dose prediction methodology is to add a filter material into the path of the beam.

The attenuation of the X-ray spectrum is dependent on three factors; the type and thickness of material used for the filter and the energy of the photons. The mass attenuation coefficient of the filter material and the density of the filter material are used in the following equation by (Beutel et al. 2000):

$$I = I_0 e^{\left(-\frac{\mu}{\rho}\right)\rho x}$$

The beam is modelled in this method using 1keV wide intervals, known as energy bins, where the number of photons that are present between 0keV-1keV, 1keV-2keV, 2keV-3keV ... 149keV-150keV are counted separately. The equation is applied separately to each energy bin, and the mass attenuation coefficient of the filter material and the density of the filter material for each of these intervals was taken from the National Institute for Science and Technology tables (NIST 1996).

The exposure is then calculated from the photon flux using the equation below (Beutel et al. 2000), where a, b and c are constants and ε is the energy of a particular bin. The total exposure is the sum of the exposure of all the individual energy bins.

$$Exposure = \frac{Photon\ Flux}{\left[a + b\sqrt{\varepsilon}\ln(\varepsilon) + \frac{c}{\varepsilon^2}\right]^{-1}}$$

The term Exposure (X) describes the amount of charge created by ionising a mass of air and is measured in Roentgen, while the entrance dose is a measure of the energy absorbed by a mass of air and is measured in Gray (usually µGy). The Exposure value can be converted to an Entrance Dose value using the following equation described previously in 2.3:

$$Entrance\ Dose\ (Gy) = 0.00876X(R)$$

The X-ray beam spectrum described by the method above is at a FSD of 1m, which is not applicable to LSSR. The 1/r attenuation rule for linear slot scanning is used to adjust the result to be suitable for LSSR (Irving et al. 2008). In order to find the entrance dose at the FSD of interest, the entrance dose is multiplied by a factor α that uses the 1/r rule to adjust FSD distance:

$$\alpha = \frac{FSD_{1m}}{FSD_{true}} = \frac{1}{FSD_{true}}$$

This method of predicting entrance dose has been validated and is used in the dose prediction studies linked to the Lodox Statscan (Irving 2008; Scheelke et al. 2005). The method was used in the static dose prediction model for the Lodox Statscan (Irving 2008), which has been adapted as described in Chapter 4.

2.5 Filtration in X-ray Imaging

2.5.1 The Effect of Filtration on an X-ray beam

Filtration is a common technique for altering the spectrum of an X-ray beam. Filtration occurs when a filter material is placed between the X-ray source and the target, reducing the number of photons reaching the target. This effect, known as "beam hardening", is depicted below in Figure 4. Some diagnostic systems are equipped with a low-atomic number filter material to absorb the low-energy photons ("soft X-rays") in the beam (Martin et al. 1999), (Martin 2007).

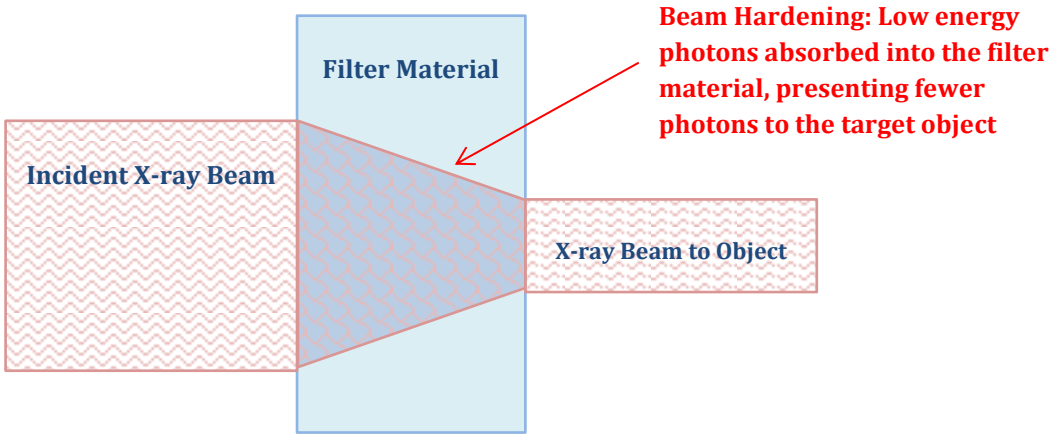

Figure 4: Incident X-ray beam photos are reduced with the addition of a filtration material.

The amount of filtration applied to an incident beam affects the image quality, as the removal of photons decreases the amount of contrast available to assess different structures in the image. Figure 5 below shows several examples of energy beam spectra under the effect of beam hardening. Water and PMMA are substances commonly used to simulate human tissue, while aluminium and copper are commonly used as filtration materials. In the figure, the graph shows tube voltages above 25kV begin to affect water and PMMA of 200mm thickness with an increase in relative number of photons, while 2mm aluminium is only affected after 30kV, and 2mm copper is only affected after 40kV. Low-energy photons do not fully penetrate the body and are absorbed in human tissue, and thus increase patient radiation dose without adding to image quality.

The aim of filtration is to block the low energy photons before they are absorbed by the human tissue, thus reducing the ionising radiation dose to patient while still providing enough photos to penetrate the human tissue fully and provide a diagnostic quality image (Martin 2007).

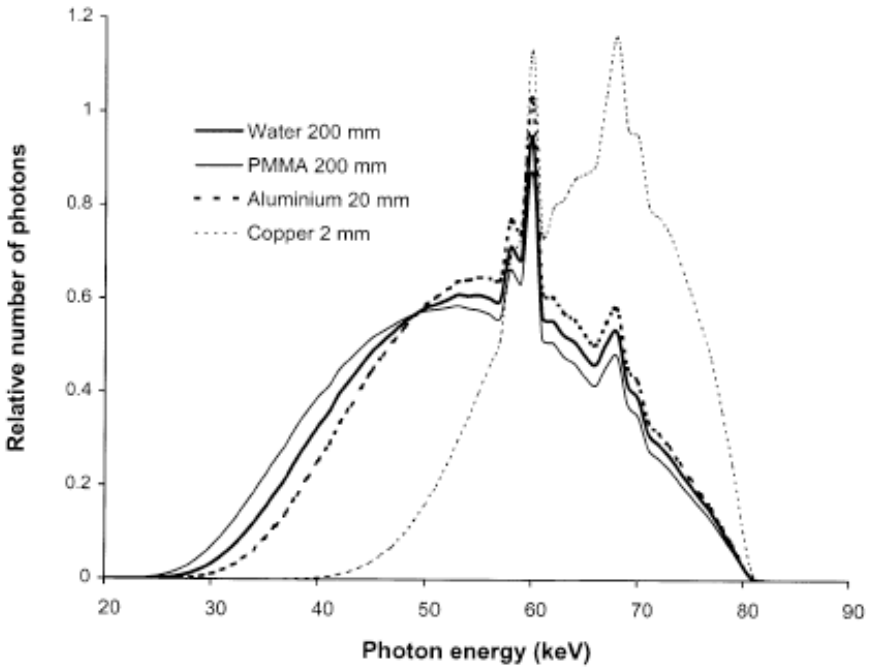

Figure 5: Graph showing effects of different materials on an X-ray beam (Martin, 2007)

Inherent aluminium filtration is standard practice in X-ray tube production (Sprawls, n.d.), while the addition of further layers of aluminium filtration has also been examined in successful studies (Behrman, 2003), (Behrman & Yasuda, 1998). Image quality to patient exposure ratio can be optimised using replacement or additional filters from the standard aluminium filters installed in some machines (Regano & Sutton 1992). The use of copper as a filter material can lower radiation dose without having a negative effect on the clinical image quality, if the tube is capable of producing the output requirements due to the increased load filtration adds to the system (Hansson et al. 1997), (Nicholson et al. 2000), (Smans et al. 2010). Insufficient beam output from the tube may induce artefacts from the filter and negatively affect image quality as well as increase exposure time (Smans et al. 2010), (Koedooder & Venema 1986). Rhodium and molybdenum have also been examined as filtration materials in studies where tube voltages are low, such as for mammography (Desponds et al., 1991; Hussein, 2008). The heavy metal, erbium, has been found to significantly reduce dose without affecting image quality in contrast abdominal images taken with conventional radiographic systems (Doyle & Brennan 1999).

The effective application of filtration to the Lodox Statscan has been described (Esterhuizen, 2010). Esterhuizen found that adding copper filtration degrades the signal to noise ratio (SNR) of the resulting images only slightly. He concluded that with less than 0.6mm copper, the image quality would not be significantly reduced.

2.5.2 Filtration in paediatric imaging

Many studies promote filtration as an effective dose-reducing technique for paediatric imaging (Brosi et al., 2011; Hansson et al., 1997; Mooney & Thomas, 1998). Brosi et al. found that copper filtration decreased the entrance-surface-dose for paediatric digital X-ray images without consistent decline in image quality. Mooney and Thomas (1998) found that 3mm aluminium filtration reduced dose, with a clinical imaging trial that showed that diagnostic image quality was maintained. The same study revealed that the attenuation provided by a 3mm aluminium filter to a 55 kV X-ray spectrum was equivalent to that provided by a 0.1mm copper filter.

Hansson et al. (1997) investigated the effect copper filtration had on digital paediatric imaging, both on radiation dose and on image quality. This study focussed on examinations with high tube voltages, between 102-105 kV. The image quality was assessed using phantoms as well as in a clinical trial. The study found that for paediatric double-contrast colon examinations, effective dose was reduced by 44% with a 0.3mm copper filter. The phantom study showed that the contrast-detail was marginally impaired by the copper filtration, while the clinical trial did not find any significant deterioration in the image quality. The copper filtration technique is now standard practice for paediatric colon examinations.

Brosi et al. (2011) examined the effect of copper filtration on paediatric examinations, specifically on image quality and dose. Dose recordings were taken using a Keithley dosimeter and the PC-based Monte Carlo program PCXMX version 2.0 was used to calculate the effective doses. The effect of filtration on image quality was assessed using a contrast-detail phantom test object. Copper filtration of 0.1mm, 0.2mm and 0.3mm were assessed. The copper filtration was found to affect the entrance dose, but in general did not affect the effective dose. The study found that there was no consistent decline in image quality relative to increased filtration, although image quality did decrease with each additional filter.

Mooney and Thomas (1998) conducted a study to optimize the radiographic technique for paediatric radiology with the end goal of reducing dose. Their clinical trial imaged paediatric patients in a dedicated paediatric room using a conventional radiography system. They assessed reduction in entrance dose as well as effective dose. Following successful preliminary examinations with phantom test objects, the clinical paediatric imaging trial found that an added filter of 3mm aluminium significantly reduced the entrance dose (51%) and effective dose (38%) without affecting image quality.

2.6 Image Quality

The objective of diagnostic medical imaging is to obtain an image of a patient which will provide sufficient information to allow the expert viewing the image to make medical decisions with a relative degree of certainty. There are many techniques for image quality verification, but the end goal should always be to provide adequate image quality for diagnosis (Martin et al. 1999). This section will examine a few of these techniques, and will highlight those that are best suited to the evaluation of LSSR digital images.

In general, quantifying image quality is very difficult (Sund et al. 2004), (Martin et al. 1999). Evaluating the image quality of diagnostic medical images is a complex task, with variations in noise level, resolution, contrast and anatomical image background affecting signal detection. The interpretation of the image also depends on the human observer, the image source and medical discipline (Båth 2010).

The recommended simple method of determining image quality is to use a test object. Test objects allow for observation of contrast differences and spatial resolution. A major benefit of using test objects is that the testing can be performed easily and regularly with a standard image, allowing for continual monitoring of image quality (Martin et al. 1999).

Although test objects are useful for determining image quality, the highest level of imaging performance verification is that of a clinical analysis. Test objects lack the anatomical relevance of a patient (Smet 2012). Images of test objects can provide an objective assessment, while anatomical image assessments are subjective to the examiner (Martin et al. 1999).

2.6.1 Qualitative Assessment

Visual grading of images by experienced radiologists is an essential part of the image analysis procedure for comparing diagnostic procedures on different systems. This is because a radiologist will have an anatomical background to identify important structures, and a subjective view of the image noise, contrast and resolution (Sund et al. 2004). Visual grading studies have high validity when images are viewed by experienced radiographers and selected based on anatomical structures (Båth 2010).

2.6.2 Quantitative Assessment

Quantitative image quality assessment focusses on the image detail from an objective standpoint, giving a quantifiable value to the test image in comparison to the control image.

Limiting spatial resolution is a quantity used to measure a system's response to small features (Martin et al. 1999), and can be tested using a line pair test object to determine the lowest resolution which the detector can determine.

Contrast is the term used in imaging to highlight the different shades of grey, light intensities and colours. The contrast sensitivity of an image is the factor which differentiates the object of focus from rest of the image (Sprawls n.d.). For the purposes of the studies outlined below, contrast is measured using a phantom test object to compare a subject test image and a baseline test image, noting the visible differences.

2.6.3 Image Quality Assessment Tools

PTW NORMI 4 FLU Test Phantoms

The PTW Normi 4 FLU ^{PLUS} test object (Figure 6) can be used to test the quality of analogue and digital X-ray installations. The phantom has a copper wedge step to measure the dynamic range, detailed contrast discs to measure high and low-level contrast constancy, as well as a line-pair tool so that spatial resolution recordings to be completed all within the same exposure. The phantom will allow for the same object to be examined under different test conditions and variations to image quality should be clearly visible.

The test object includes an attenuation plate to simulate a patient in the X-ray beam path. The threshold contrast percentage is the smallest change in contrast of luminance (or brightness) that can be perceived by the human eye, and is recorded by observing the number of visible contrast discs on the X-ray image compared to the number of contrast disks available.

The three contrast values are:

- Number of copper wedge steps visible
    - 17 blocks are available to rate the dynamic range
- Number of 10 mm diameter contrast-detail inserts visible (large discs)
    - 8 large discs available to score
- Number of 4 mm diameter contrast-detail inserts visible (small discs inside blocks)
    - 16 small discs available to score

Figure 7 below shows an X-ray image of the PTW Normi 4 FLU ^{PLUS} test object.

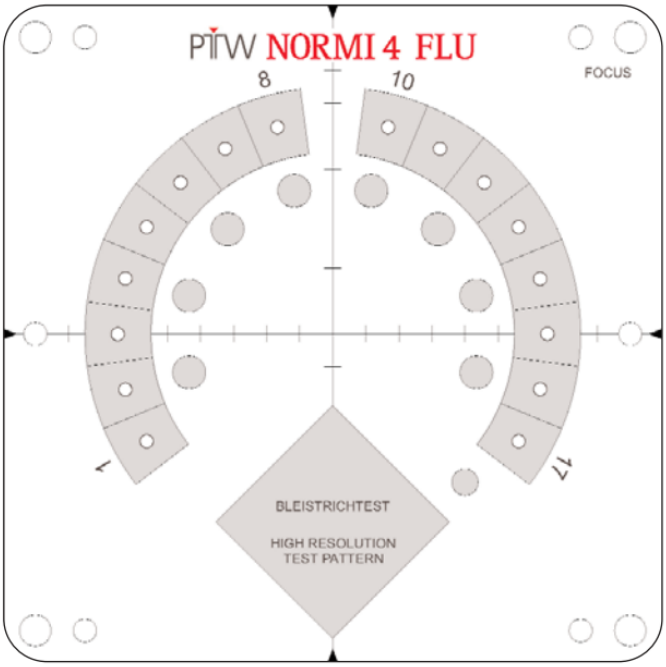

Figure 6: PTW Normi 4 FLU^{PLUS} test object [www.ptw.de] with different areas for assessing contrast and resolution.

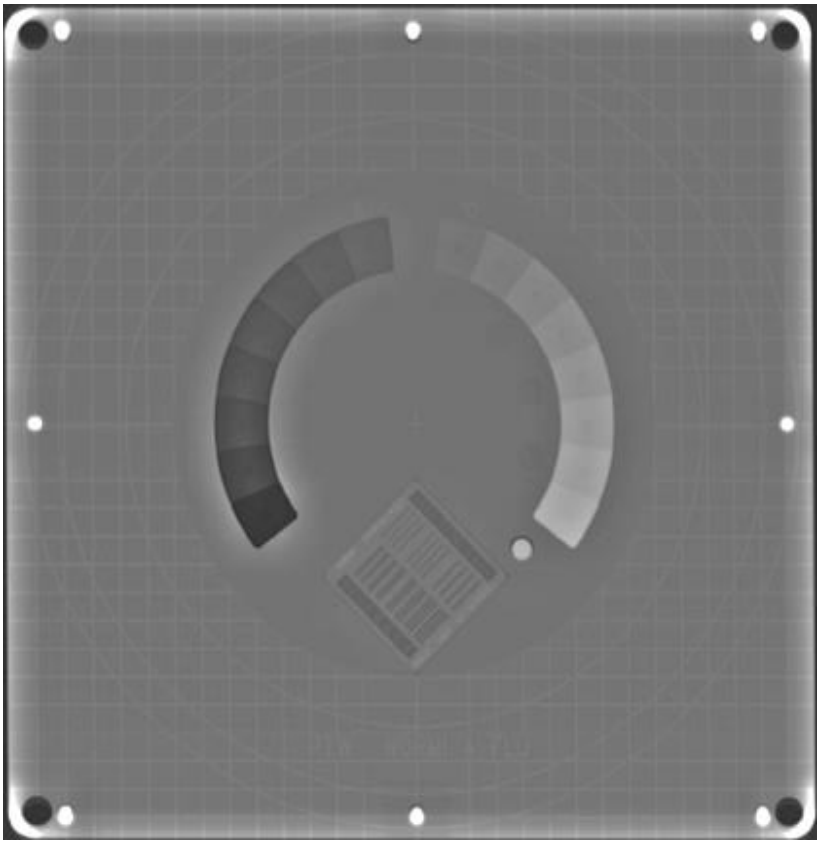

Figure 7: An X-ray image of the PTW Normi 4 FLU^{PLUS} test object

2.6.4 Alderson RANDO Phantom

The Alderson RANDO phantom is constructed with human appearance, and contains a natural human skeleton surrounded by a material that is equivalent to human tissue, and thus the overall effect is similar to that of a human skeleton when scanned. X-ray images of the RANDO phantom provide a good simulation of human conditions for dose recordings, but lack the anatomical detail for diagnostic image quality testing. Figure 8 shows the phantom alongside an X-ray image of the chest section. The Alderson RANDO phantom is versatile in that it can be separated into slices for different specific imaging studies.

Irving et al. (2008) examined dose reduction for LSSR using the Alderson Rando phantom to simulate a human chest, abdomen and pelvis. The study measured entrance dose for AP examinations.

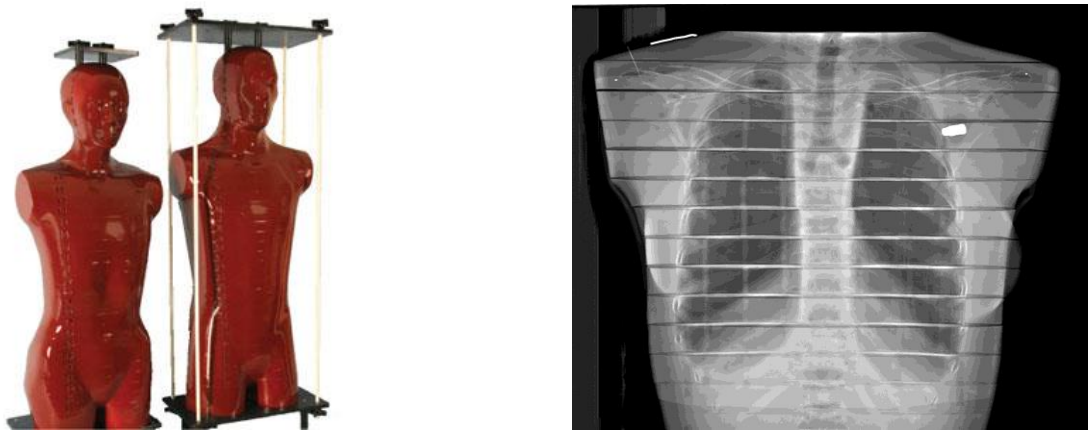

Figure 8: Alderson RANDO Phantom [www.rsdphantoms.com] and an image of a chest X-ray of the phantom

2.6.5 Visual Grading in Clinical Imaging Studies

Hamer et al. (2005) assessed the image quality maintenance in chest/lung images when a copper filtration technique was implemented on a digital imaging system. They made use of a visual grading scoring system, originally based on the European Guidelines on Quality Criteria for Diagnostic Radiographic Images, for assessing the anatomical and subjective viewing quality of the image. In that study, experienced radiologists examined 100 chest/lung digital X-ray images and scored them independently according to personal interpretation. The images were screened at random, and the viewer did not have knowledge as to which images had the added copper filtration and which did not. The scoring system rated each image on a numerical scale from “excellent visualization” (score of 1) to “poor visualization” (score of 7), where “moderate visualization” (score of 5) was the threshold where diagnostic viewing capability was limited. The viewing radiologists shared an agreement of 99.7% in their opinion of the images reviewed, and found that the image quality was maintained for all images assessed. The study found that dose was reduced and image quality was maintained with the implementation of the proposed filtration technique.

A similar 7-point scoring system for visual grading of images was used at the University of Cape Town (Irving et al. 2008) for a study on the Lodox Statscan. The study compared digital X-ray images captured on the Statscan with images captured using a conventional radiography system. The study found that the same amount of visual information was present using the Statscan as with conventional radiography in the antero-posterior (AP) plane. The study suggested that the LSSR system could replace conventional radiography due to the lowered dose and maintained image quality.

2.6.6 Detector Quantum Efficiency

Detector Quantum Efficiency (DQE) is the term used to describe the efficiency of an imaging detector, compared to an ideal detector. DQE is an analysis of signal information and does not take into account the effect image processing has on an image and the limited visual observations a human can make from an image; it specifically looks at the raw data from the detector.

DQE as a measure of signal-to-noise ratio (SNR) is applicable to any imaging system and can be used to compare detectors of various systems provided the anatomical background is not taken into account (Båth 2010; Scheelke et al. 2005). The high DQE of digital systems allows images to be recorded at a much lower dose (Busch & Faulkner 2005). X-ray systems which use flat panel detectors to record the image have shown that they produce similar quality images while offering a lower radiation dose compared to standard conventional X-ray which captures the X-ray image directly onto film. This is due to the high DQE that is offered by flat panel detectors (Szucs-Farkas & Vock 2009).

Although DQE can be used as an effective technique for evaluating the intrinsic performance or digital X-ray systems, it has two limitations which make it fall short as a method of measuring the overall performance of a radiologic imaging system: (a) DQE evaluates the detector relative to primary X-ray radiation, without the presence of a scatter medium (patient/phantom), and (b) the DQE is often a measure of the detector performance in itself, without taking into account the other imaging factors such as an antiscatter grid or air gap (Samei et al. 2005). A “system DQE” has been suggested as a method of comparing overall performance of different radiography machines, which includes scatter radiation and other elements (Scheelke et al. 2005).

2.7 Summary

This literature review has highlighted the following regarding dose and filtration:

- A dose prediction model for LSSR has been developed and validated.
- Filtration is a well-known method to reduce dose to patient, with image quality as the major trade-off.
- Filtration techniques specific to the Lodox Statscan have not been investigated thoroughly, nor has the current 0.1mm copper filtration technique been validated.

3. Validation of Existing 0.1mm Copper Filtration on Dose and Image Quality

3.1 Introduction

The literature describes filtration as a successful technique for reducing radiation exposure in radiographic imaging (Brosi et al. 2011; Behrman & Yasuda 1998; Smans et al. 2010; Hansson et al. 1997). This chapter describes the validation of a 0.1mm copper filtration technique currently installed on the Lodox Statscan for all standard high voltage scans. The purpose of the filtration is to reduce the ionising radiation dose to the patient, while maintaining diagnostic image quality.

3.2 Methods

The use of a 0.1mm copper filter is standard on all Lodox Statscan examinations requiring a tube voltage over 110kV. Prior to this study, the effect of this copper filtration on the quality of the image had never been formally examined. The Lodox Statscan has a solenoid build into the collimator, which inserts a 0.1mm copper filter into the X-ray beam path automatically when a scan requiring a tube voltage higher than 110kV is selected. For the purposes of this study, the Statscan at the University of Cape Town was set for manual solenoid activation, to allow for readings at high kV settings with and without the filter inserted.

The following series of studies were performed to assess the 0.1mm Cu filtration:

Dose measurement

The PTW UNIDOS dosimeter was used together with a 30 cc, 300V PTW ionization chamber to record entrance doses in this study. The dose is recorded in µGy. The calibration certificate of the PTW dosimeter assures accuracy to within 5% of the measured value. All measurements were taken free-in-air. Correction for ambient temperature and pressure was added to the measured doses as the automatic correction factor was de-activated. These environmental factors were recorded for each scanning session and applied to the relative dose readings.

The standard settings on the Lodox Statscan for extra-large patients make use of tube voltages higher than 110kV. Each of these “X-Large” settings was assessed for dose reduction and image quality maintenance.

The dosimeter was scanned twice for each setting, once with the copper filter applied and once without. The doses were recorded for comparison. Correction for ambient temperature and pressure was added to the measured doses. To evaluate the effect that the filtration would have in a clinical setting, the effective doses were calculated from the recorded entrance doses. The effective doses were obtained from the entrance doses using the PCXMC (Version 2.0) Monte Carlo code for the appropriate large sized theoretical patient.

Image quality assessment

Image quality is the major trade off when lowering radiation (Slovis, 2002). The Normi 4 FLU^{PLUS} test object was selected to provide comparative assessments with and without added filtration. Changes in contrast and spatial resolution were recorded using the Normi 4 FLU^{PLUS} test object, which gives a numerical value to the contrast and spatial resolution. These figures were used as metrics for assessing whether the filter affected the image quality, as described in the literature review. The images were assessed visually by the author, a medical physicist and an experienced clinical radiographer. The three observers viewed the images together as a panel throughout the study, and conferred about each image assessed.

The Alderson Rando phantom and large cadaver specimens were also used for image quality assessment, as these methods provide images with anatomical backgrounds for an insight into the clinical application of the filtration technique. These images were assessed visually by an experienced clinical radiographer.

The PTW Normi 4FLU^{PLUS} test object was placed on the Lodox Statscan scanning table and imaged for the range of standard "X-Large". For each scan setting, the test object was imaged with and without filtration. The spatial resolution (line pairs) and threshold contrast (blocks, large discs, and small discs) were reviewed. A description of how the phantom quantifies the image quality is given in 2.6.3.

The Alderson RANDO test object was used to assess the image quality maintenance of basic anatomical structures with the addition of copper filtration. The Lodox Statscan standard settings for the extra-large chest, abdomen and pelvic examinations were used. For each scan setting, the test object was imaged with and without filtration. This phantom is described in 2.6.4.

A series of cadaver images were scanned to assess the image quality maintenance of more detailed anatomical structures with the addition of copper filtration. The University of Cape Town has access to whole cadavers and cadaver specimens for medical research. Ethics approval was obtained for X-ray imaging examination of cadavers on the Lodox Statscan. A very large torso was examined under the extra-large standard settings on the Lodox Statscan. Standard extra-large chest, abdomen and pelvic examinations were imaged. For each scan setting, the test object was imaged with and without filtration.

3.3 Results

3.3.1 Dose Reduction with 0.1mm Copper Filtration

A 0.1mm copper filter was tested in a study to examine the effects of filtration on the different standard settings given to each high tube voltage examination available on the Lodox Statscan (above 110kV). Technique factors for each standard examination available within the Lodox Statscan which makes use of high tube voltages was examined with and without the 0.1mm copper filter. The available Statscan adult examinations and the resultant doses with and without filtration can be seen in Table 1. Only anterior-posterior (AP) examinations were considered in this study.

The average resultant decrease in effective dose for standard Statscan examinations above 110kV was found to be 25.82%, with the maximum reduction being 29.0% (skull) and the minimum reduction being 22.7% (abdomen).

Table 1: Entrance and effective dose reduction with a 0.1mm copper filter on high voltage scans on the Lodox Statscan; the tube voltage and current settings are determined by the system for the chosen examination. Only anterior-posterior scans were taken.

Procedure Name and Patient Size	Tube Voltage [kV]	Tube Current [mA]	Entrance Dose without 0.1 mm Cu Filter [µGy]	Entrance Dose with 0.1 mm Cu Filter [µGy]	Effective Dose without 0.1 mm Cu Filter [mSv]	Effective Dose with 0.1 mm Cu Filter [mSv]	Percentage Dose Reduction [%]
Chest (lung) Extra Large	140	160	315	200	0.114	0.084	**26.7**
Full Body (Abdomen) Large	120	160	131	78	0.106	0.077	**27.5**
Full Body (Abdomen) Extra Large	145	200	222	147	0.190	0.147	**22.7**
Abdomen Extra Large	120	200	891	548	0.228	0.176	**23.2**
Pelvis Extra Large	120	200	913	544	0.159	0.118	**25.7**
Skull Extra Large	120	200	329	190	0.008	0.006	**29.0**

3.3.2 Effect on Image Quality with 0.1mm Copper Filtration

The effect that 0.1mm copper filtration has on the image quality for the Lodox Statscan was assessed for high tube voltage examinations on the Statscan, as this is the current standard setting for which the filter is applied.

PTW Normi 4FLU^{PLUS} Phantom for high tube voltages

Table 2 below summarises the examinations reviewed, and the resultant spatial resolution and contrast values. The comparison found the image quality to be identical with and without the added copper filtration, with the exception of the pelvic examination. For the pelvic examinations, the contrast was found to be minimally affected, while the spatial resolution was found to be identical.

The baseline image of the PTW phantom for the standard Full Body AP examination on the Lodox Statscan for a large patient can be seen in Figure 9. Figure 10 is the image of the phantom with the 0.1mm copper filtration applied. When reviewing these two images independently in the Lodox DX digital imaging software, they were found to be equivalent. With the exception of the pelvic examination, the other examinations were found to be unchanged with the addition of the copper filtration

Table 2: Image quality comparison for high kV examinations on the Lodox Statscan with and without 0.1mm copper filtration using the PTX Normi test phantom

Procedure Name and Patient Size	Tube Voltage [kV]	Tube Current [mA]	Phantom Image Quality without 0.1 mm Cu Filter				Phantom Image Quality with 0.1 mm Cu Filter			
			Line Pairs	Contrast			Line Pairs	Contrast		
Chest (lung) Extra Large	140	160	2.2	17	5	15	2.2	17	5	15
Full Body (Abdomen) Large	120	160	2.0	17	5	16	2.0	17	5	16
Full Body (Abdomen) Extra Large	145	200	1.6	17	4	15	1.6	17	4	15
Abdomen Extra Large	120	200	2.2	14	5	11	2.2	14	5	11
Pelvis Extra Large	120	200	2.2	14	5	11	2.2	14	4	11
Skull Extra Large	120	200	2.8	17	5	16	2.8	17	5	16

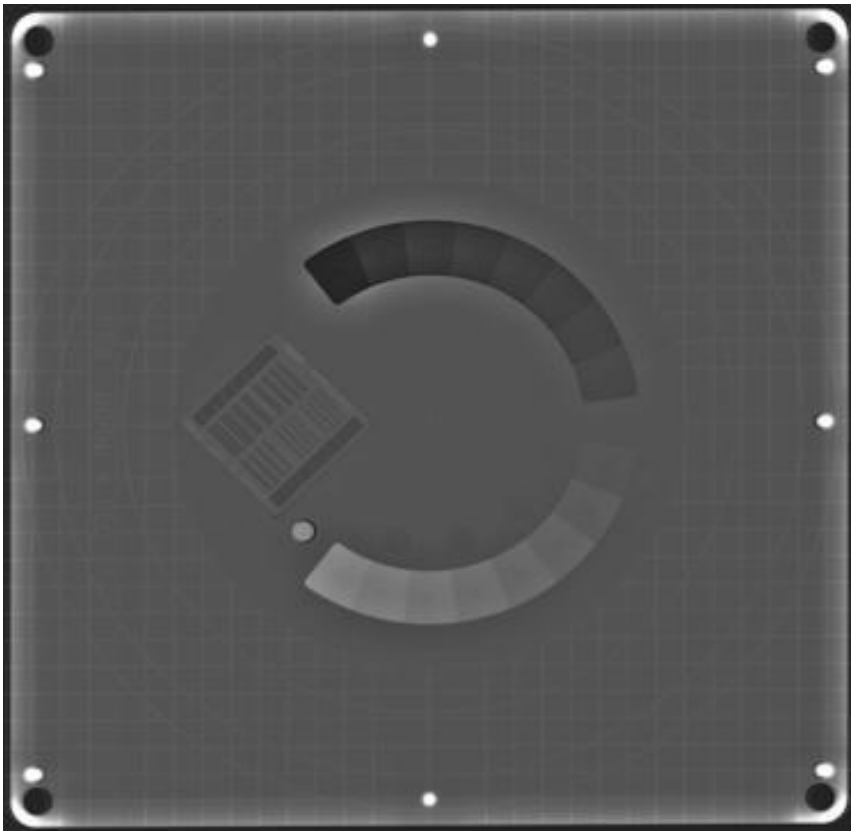

Figure 9: Phantom image at 120 kV, 160 mA (Large Full Body AP) without 0.1mm Cu Filter

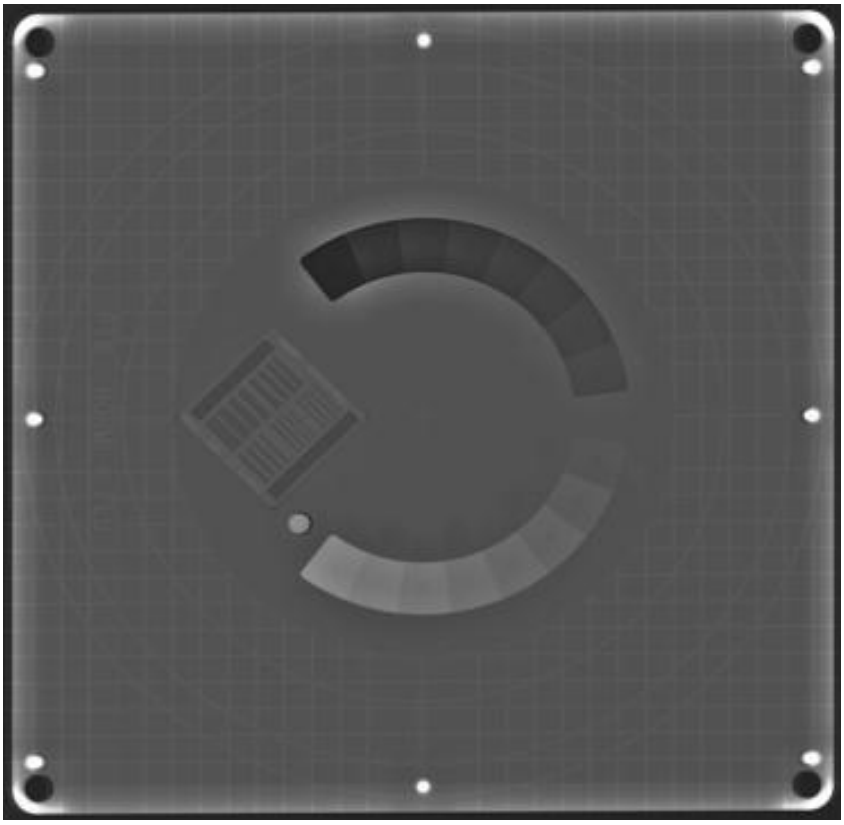

Figure 10: Phantom image at 120 kV, 160 mA (Large Full Body AP) with 0.1mm Cu Filter

Alderson RANDO Phantom Test

The unfiltered image of the standard chest X-ray for an extra-large patient can be seen in Figure 11, while Figure 12 shows the same test object with 0.1mm added copper filtration. The images were assessed by an experienced clinical radiographer, who found that both images highlighted the same anatomical structures with diagnostic quality. The bifurcation of the trachea can be seen clearly, as well as the bone structures throughout the image.

Similarly, for the abdominal and pelvic examinations, the radiographer confirmed that when comparing the phantom's available anatomical structures pre and post filtration, the images were not affected by 0.1mm added copper filtration.

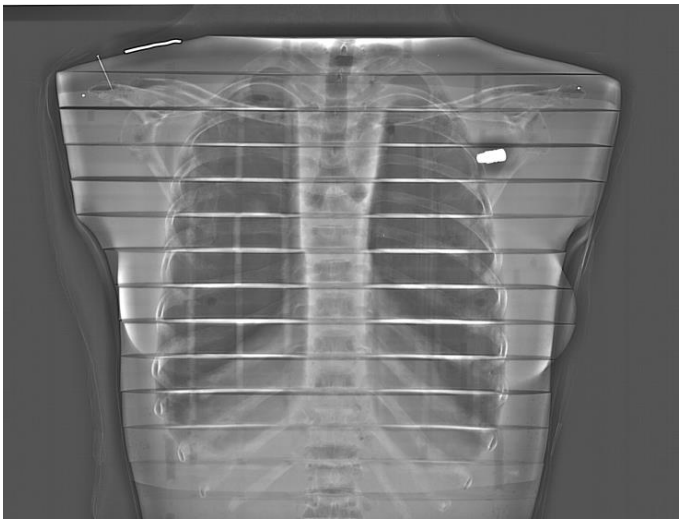

Figure 11: Standard X-Large chest X-ray of the Alderson RANDO phantom without added copper filtration

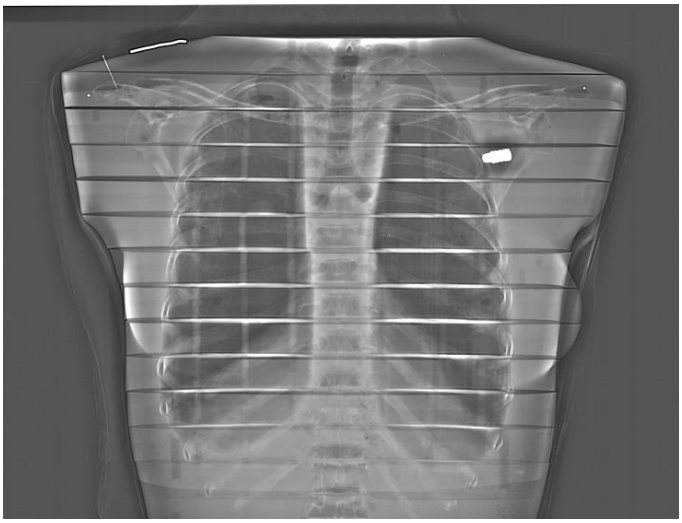

Figure 12: Standard X-Large chest X-ray of the Alderson RANDO phantom with 0.1mm added copper filtration

X-Large Cadaver Test

The unfiltered image of the standard chest X-ray for an extra-large patient is shown in Figure 13, while Figure 14 shows the same object imaged with 0.1mm added copper filtration. The images were assessed by an experienced clinical radiographer. Both images highlighted the same anatomical structures with diagnostic quality.

A slight difference in the contrast of the image was noted following the addition of the filter material, but this did not negatively affect the viewing of relevant anatomical structures within the image. By making use of the digital imaging viewing tools available, a slight manipulation of the window and level settings within the diagnostic software made the two images indistinguishable. The embalming fluid used to preserve the cadaver may have impacted the viewing conditions.

Figure 13: X-Large cadaver chest, unfiltered

Figure 14: X-Large cadaver chest, filtered 0.1mm Cu

Similarly, the abdominal (Figure 15 and Figure 16) and pelvic (Figure 17 and Figure 18) examinations confirmed that anatomical structures are not affected by 0.1mm added copper filtration for the high tube voltage examinations of the Lodox Statscan.

Figure 15: X-Large cadaver abdomen, unfiltered

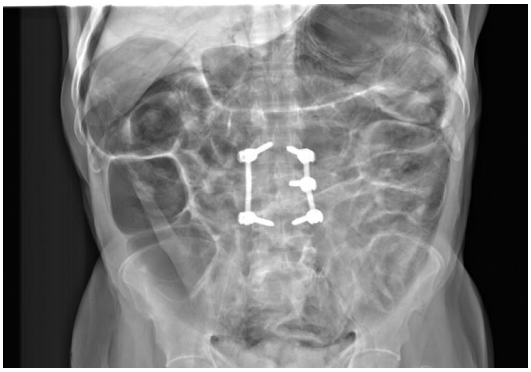

Figure 16: X-Large cadaver abdomen, filtered 0.1mm Cu

Figure 17: X-Large cadaver pelvis, unfiltered

Figure 18: X-Large cadaver pelvis, filtered 0.1mm Cu

3.4 Conclusion

A 0.1mm copper filter is already standard to the Lodox Statscan, and the filter is automatically applied to scans where the tube voltage is in excess of 110kV. The use of this filter has been validated: it has been found to reduce dose without compromising image quality.

4. Development of a Dynamic Dose Prediction Model

The need to lower the radiation dose from X-ray imaging to patients and employees has been established in the reviewed literature, which also suggests that dose can be reduced by the addition of a filter material into the beam of the X-rays to eliminate the lower energy X-rays.

This chapter describes the adaptation of Irving's (2008) static dose prediction model. The static model was used as the basis for the development of a new dynamic dose prediction model. The goal was to develop a user interface which allowed the user to vary the Statscan scanning parameters, the filter material and the thickness of the filter material in order to examine the effect on the beam spectrum and the expected dose. The purpose of the dynamic model was to assist in the development of new filtration techniques for the Lodox Statscan.

4.1 Static Dose Prediction Model

The static dose prediction model previously developed by Irving (2008) is described in further detail below. The model takes an input set of technique factors for a particular X-ray procedure, and then generates a simulation energy spectrum which models the expected X-ray beam spectrum. The model attenuates the simulated energy spectrum by placing a theoretical filter material in the path of the beam. The final entrance dose is calculated using the attenuated simulation energy spectrum. The energy spectrum can further be applied to the energy absorption data for a standard sized patient to calculate the effective dose to a standard sized patient. This model has been validated, and computes faster than similar Monte Carlo simulations (Irving 2008).

4.1.1 Function-Flow Static Dose Prediction Model

Irving's (2008) dose prediction model algorithms were developed in Matlab.

The input technique factors used to obtain the image are used directly in a beam spectrum generation algorithm, and the expected entrance dose can be calculated directly using this algorithm. Effective dose prediction calculation requires the patient size dimensions as input parameters in order to use the ICRP103 energy absorption weighting factors in order to accurately predict the collective effective dose to patient. The input parameters are given below.

Input technique factors:

- Tube voltage - kV
- Tube current - mA
- Scanning speed - mm/s
- Source-to-skin distance - mm
- Source to collimator distance - mm
- Collimator width - mm
- Thickness of added filtration – mm

Input patient dimensions:

- Height - cm
- Weight - kg

Photon/Organ energy absorption coefficients:

- Weighting factors for each organ (ICRP 2007)
- PCXMC organ masses for a standard patient

4.1.2 Output from the Static Dose Prediction Model

Data Output

The static model output estimates the entrance dose and the effective dose for the given input parameters, as well as giving the time the calculation took to complete. Figure 19 shows a dose prediction flow diagram for the static model. The model provides an output text file (Figure 20) which displays the input parameters as well as the output predictions.

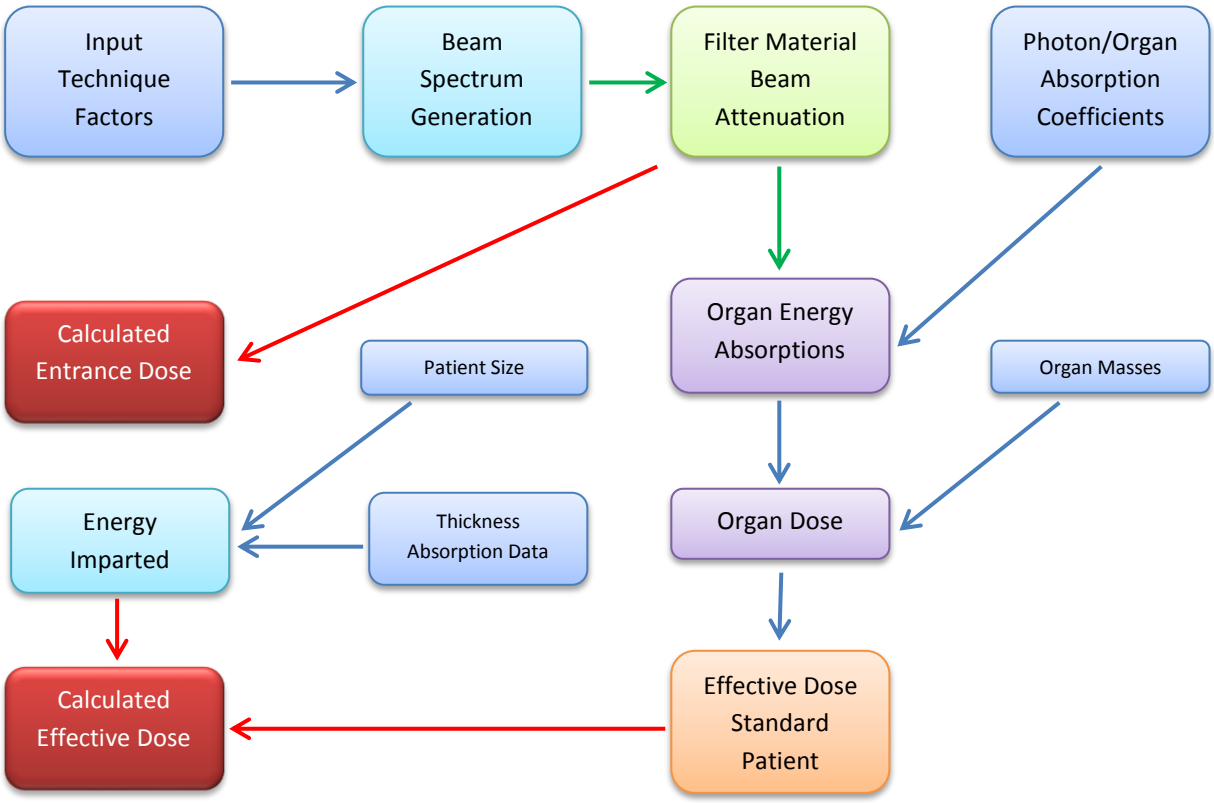

Figure 19 Function flow diagram of the static dose prediction model

```
Parameters of the examination
       M0: 71.1000
       h0: 174
    Area0: 4000
       Z0: 190
        M: 130
        h: 200
     Area: 5.7988e+03
        Z: 239.6349

          kV1: 100
          mA1: 200
       speed1: 70
         SSD1: 980
    colwidth1: 0.4000
           SC: 400
    filthick1: 1
          mAs: 2.8000
     half_val: 4.1000
    half_val2: 4.0000

Entrance Doses estimations 1 and 2 (uGy)
  250.8179  256.6341

Effective doses for standard patient and specified patient (mSv)
    0.0828    0.0695

Elapsed time is 3.663398 seconds.
```

Figure 20: Output results in text format from static dose prediction model.

Graphic Image Output

The static dose prediction model also produces three output screens with images displaying information relative to the input scan parameters, the beam generated, the attenuation of the beam, and the effective dose relative to the organs.

Output Beam Spectrum

The energy spectrum generated for the given input variables is shown in the image below in Figure 21. The spectrum displays the total number of photons, in 1keV wide energy bins, that move through a cross-sectional area of 1mm^2. The entrance dose estimation is given in the text output (Figure 20).

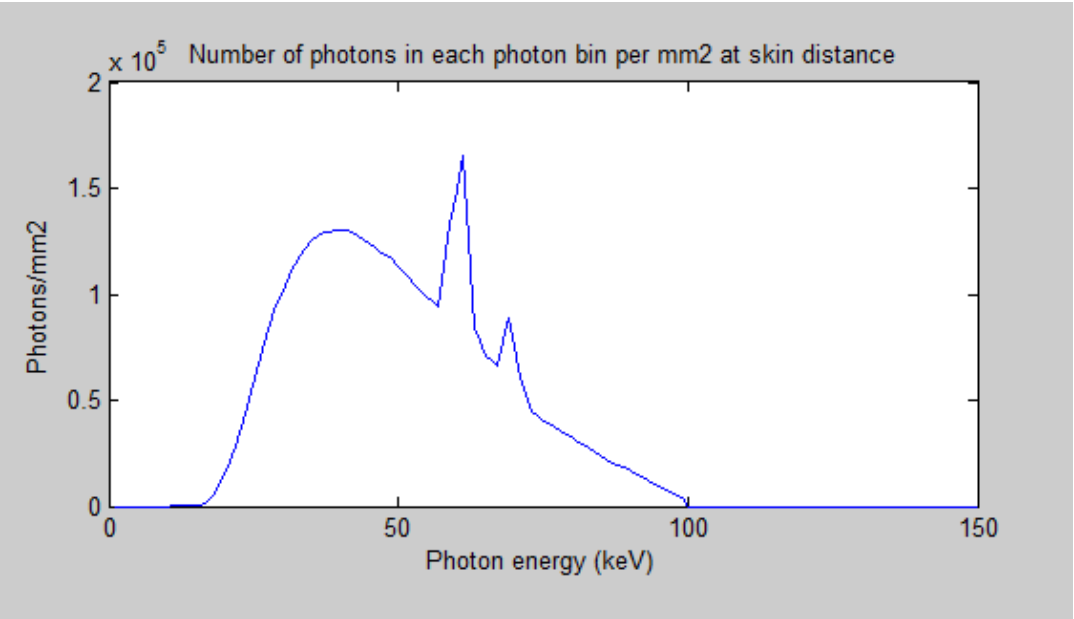

Figure 21: Example of the energy spectrum predicted by the static dose prediction model.

Effective Dose Per Slice

The graph depicted in below displays the predicted effective dose throughout the scan length. The scan length is divided up into slices over the length of the body. This graph highlights the segments of the scan which have a greater contribution to the total effective dose; the peak slices are organs which are more sensitive to radiation according to the ICRP. The blue line shows the effective dose estimates for a standard size patient, while the green line shows the effective dose estimate of the patient size dimensions entered into the model (in this case a paediatric patient, showing a higher organ dose impact).

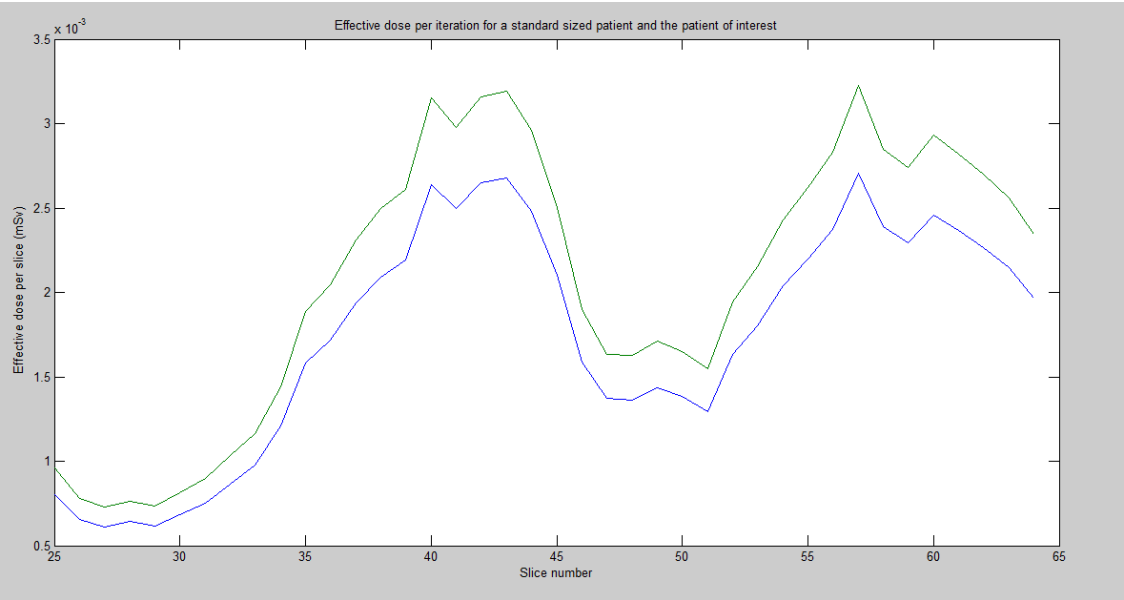

Figure 22: Example of the predicted effective dose for each slice of the scan length for the static dose prediction model, for a standard size patient (blue) and a paediatric patient (green).

Effective Dose to Each Organ

The graph shown in Figure 23 displays the effect that the predicted effective dose per slice has on each of the organs throughout the scan length. The equivalent dose is the average dose to each organ, calculated by dividing the energy which the organ absorbs during the scan by the mass of the organ (relevant to patient size). From the graph, one can see which organs are likely to be highly affected by the scan. If a high-dose-zone is not critical to the imaging needed, radiation protection measures (such as using a lead shield) can be taken to protect those organs.

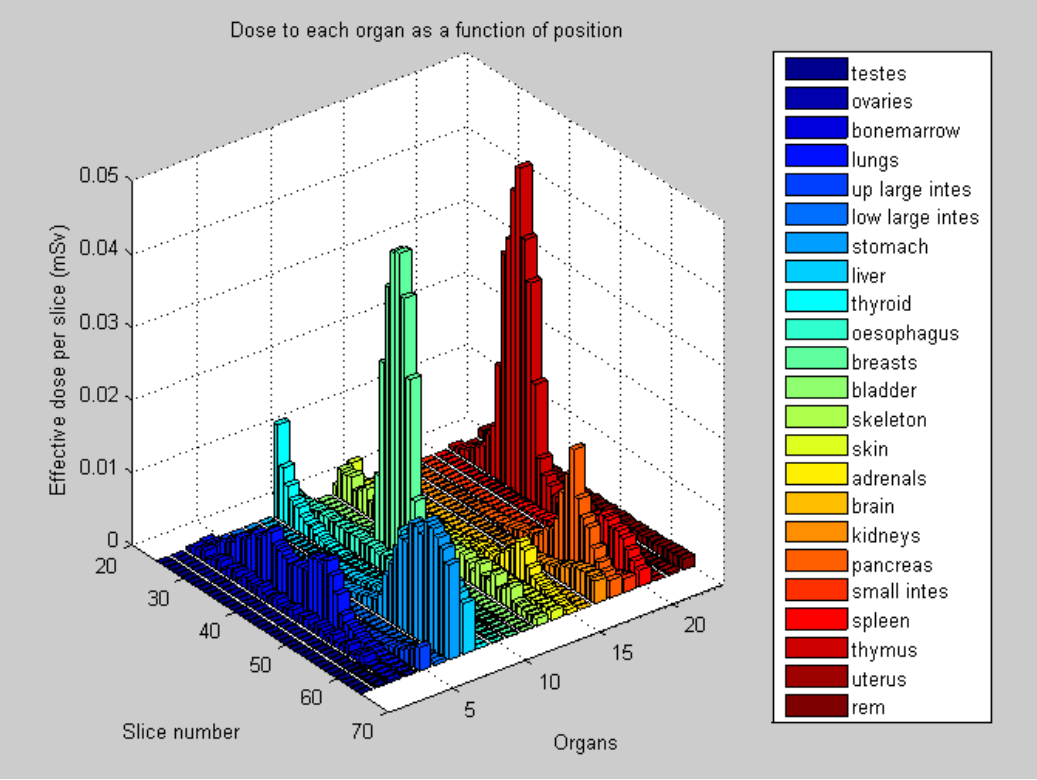

Figure 23 Separate output image showing dose predicted for each organ through a whole body scan.

4.1.3 Limitations of the Static Dose Prediction Model

The static dose prediction model has been verified against existing dose prediction models and also against measured results and it has been tested on the range of examinations for the Lodox Statscan (Irving 2008). This includes the full Statscan range of tube voltages, tube currents, scanning speeds and other input technique factors. The static dose prediction model has some advantages over other similar models in that it can calculate effective dose for any given tube voltage, and it accounts for sensitive organs when calculating the effective dose.

The major shortcoming of this dose prediction model is that there is not a simple method to alter the input parameters. For each different scenario that is to be modelled, the hard code needs to be altered to insert the input parameters for that scenario. This static model only accounts for aluminium as a filter material, which limits its functionality for comparing dose predictions. The output graphs for the static model are displayed in separate windows which limits the ease of reviewing the results.

The extension of this model into a more dynamic one, where input parameters can be varied with ease and the output is displayed to provide a comprehensive overview of the results, was desirable.

4.2 A Dynamic Dose Prediction Model

The static dose prediction model described above was designed, developed and validated for one particular set of input parameters. The aim of the dynamic dose prediction model is to allow for a wider range of input parameters to be applied to the model and to show the resultant outputs of for each variation immediately. This section describes the design and development of a dynamic version of the dose prediction model.

4.2.1 Design Principles

The primary objective of the dynamic dose prediction model was to calculate the patient entrance dose and effective dose from an energy spectrum generated using the input parameters. The input parameters should be variable, within the constraints of the Lodox Statscan standard settings, and should enable the selection of the best parameters based on predicted dose over a range of parameters. The second objective was to increase the number of filtration materials available to attenuate the energy spectrum. The third objective was to improve the speed and presentation of the model, producing faster results with an easier to use graphic user interface (GUI). The fourth objective was to display the relevant information a simple and user-friendly way.

4.2.2 Implementation

The code for the static model was adapted to allow for the technique factors associated with the beam spectrum generation and effective dose calculations to be altered according to the needs of a specific examination for which the predicted dose is needed.

The GUI screen was designed to allow for adjustments to any and all of the input variables. Figure 24 displays how the input parameters can be changed, with descriptions alongside.

Input technique factors:

Scan orientation

The Statscan has the ability to scan in the antero-posterior (AP) or lateral (LAT) orientations. A drop-down list is used to make the selection.

Tube voltage – kV

A slider bar was used to allow for simple tube voltage selection in the range from 40kV to 140kV. The steps are in 10kV increments.

Tube current – mA

The Statscan has a variety of standard tube current factors relative to their standard scan settings. These tube currents are listed in a drop-down list for selection.

Source-to-skin distance – mm

The source to skin distance is measured from the focal spot on the X-ray tube to 2mm before the X-rays make contact with the patient skin. This amount, measured in mm, is input into a textbox.

Source to collimator distance – mm

The source to collimator distance is measured from the focal spot on the X-ray tube to the collimator, where the beam spectrum is aligned and where the added filtration takes place. This amount, measured in mm, is input into a textbox.

Collimator width – mm

The collimator width sets the width of the X-ray beam to which the patient is exposed. The Statscan only allows for certain collimator widths, presented here in a drop-down list.

Scanning speed - mm/s

The Statscan allows for three scanning speeds: quarter speed, half speed and full speed. The speeds are measured in millimetres per second, and are listed in a drop-down list.

Body Position

Although the Statscan is a full-body scanning system, it also allows for scans of specific regions of interest. The dose prediction model allows for the body to be separated into segments: full body, head, chest or abdomen/pelvis. These options are listed in a drop-down box.

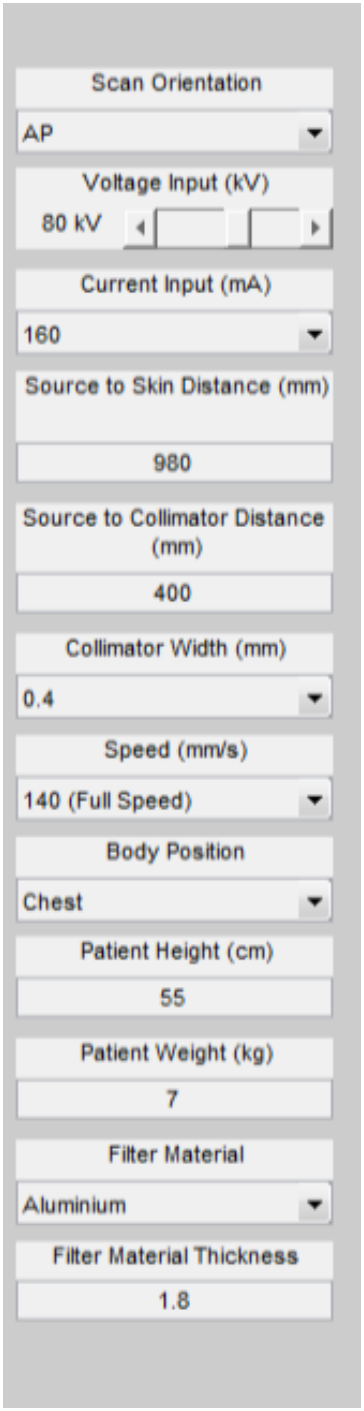

Figure 24: Input variables

Patient height (cm) and weight (kg)

The patient height and weight are entered into separate text boxes. The weight in kilograms is used in the calculations for effective dose, while the height in centimetres is used to divide up the scan slices into the correct segments (i.e. head, chest, abdomen/pelvis).

Filtration material

Filtration materials are listed in a drop-down list: aluminium, copper, rhodium, molybdenum, gold, silver, tin, lead and brass. Selecting the material will cross-reference the mass attenuation coefficient and density constant applicable for that material at the tube voltage selected above. These coefficients and constants were

taken from the National Institute of Science and Technology (NIST) X-ray Attenuation Databases found on their website (NIST 1996).

Filtration material thickness

The thickness of the selected filter material is entered into a text box; the unit of measurement is millimetres. The thickness of the material, as well as the material itself, will determine the extent of the attenuation of the X-ray beam.

Output display

The static model output included four graphs displayed in three separate windows, as well as several text outputs which were displayed in the Matlab workspace. For the dynamic dose prediction model, the graphical output images are displayed together in the centre of the screen, with the text outputs displayed on the right hand section of the screen.

The four output graphs for the dynamic dose prediction model are combined to be viewed simultaneously on the output screen. Each time an input factor is changed, the output images automatically update to display the corresponding information depicting the predicted beam spectrum and effective organ doses.

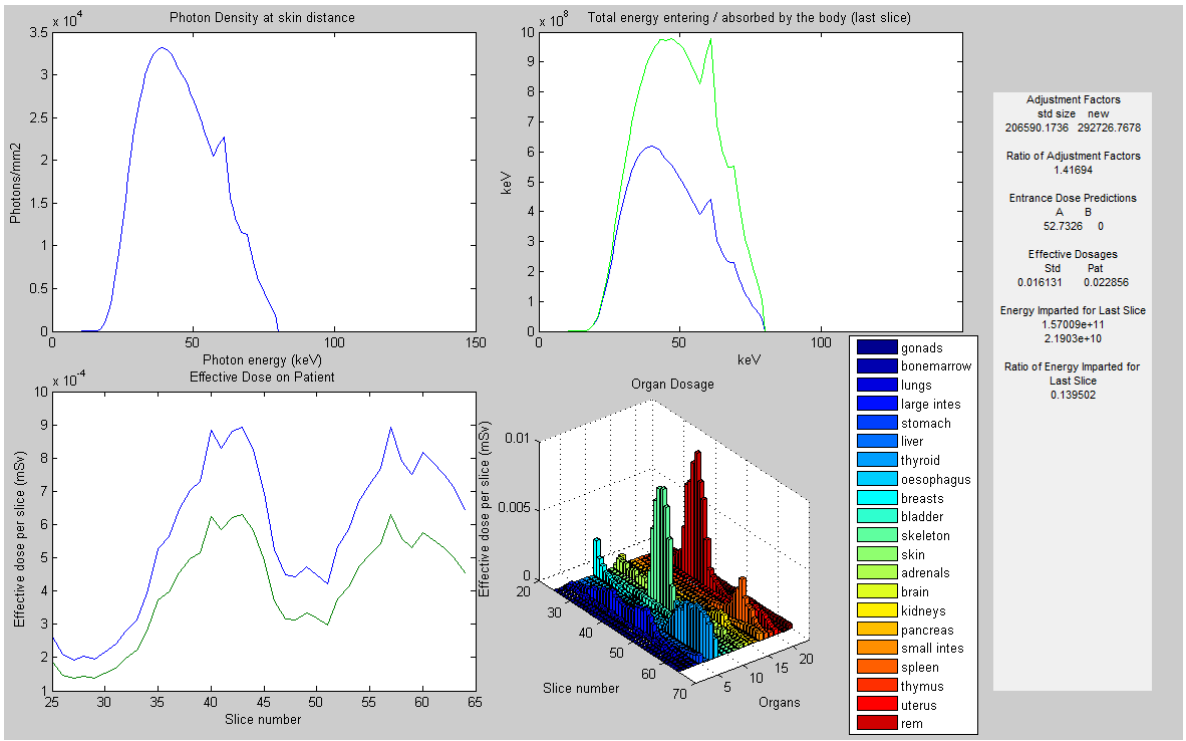

Figure 25: GUI output display for a paediatric chest simulation. The blue line shows estimates for a standard size patient, and the green line for the patient size dimensions entered into the model.

The output text displayed on the right of the dynamic dose prediction model GUI (see Figure 25) shows the expected entrance dose and estimated effective dose, relative to the input parameters.

Full GUI

The completed GUI (see Figure 26) places the input variables on the left-hand side of the screen, the output image data in the central portion of the screen, and the output text data is displayed on the left-hand side of the screen.

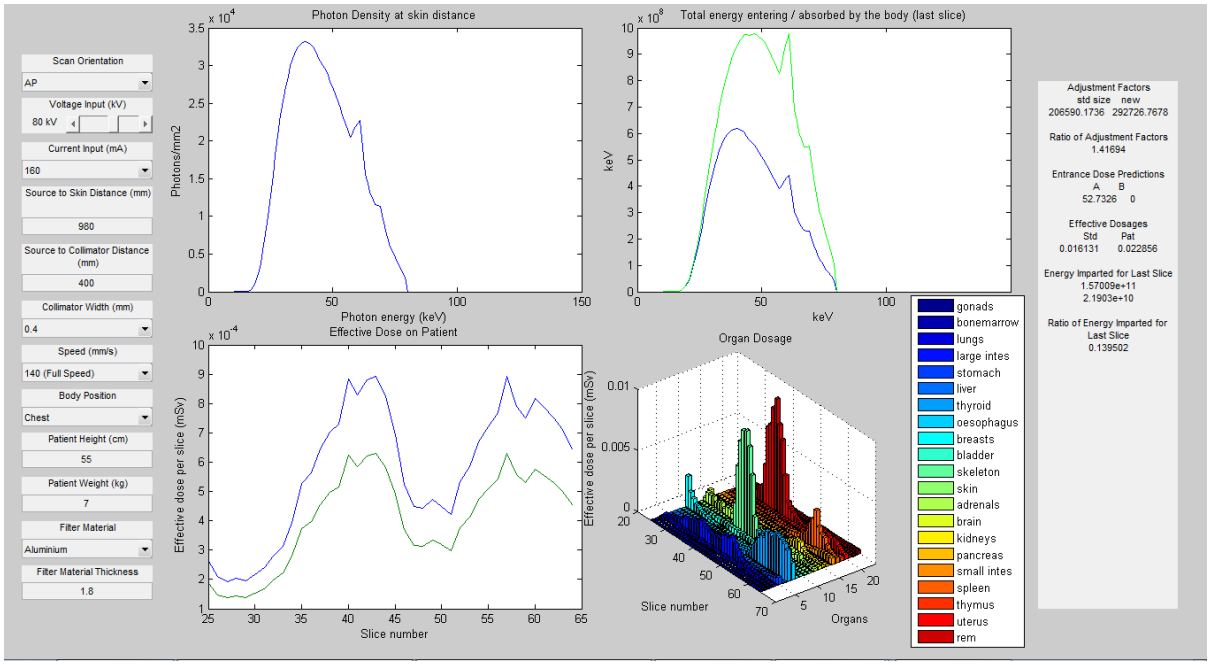

Figure 26: GUI for the dynamic dose prediction model.

4.3 Testing the Dynamic Dose Prediction Model

The dynamic dose prediction model was used to predict entrance dose for the standard paediatric examination settings on the Lodox Statscan. The predicted skin entrance doses were recorded for a range of known filter materials and relative thicknesses. The aim was to select filters suitable for dose reduction.

These standard settings are:

- Scan orientation - Anterior-posterior (AP)
- Tube voltage – 80kV
- Tube current – 160mA
- Source-to-skin distance – 980mm
- Source to collimator distance – 400mm
- Collimator width – 0.4mm
- Scanning speed – Full speed
- Body Position – Full body scan
- The PCXMC Monte Carlo simulator describes the standard paediatric patient (aged 5 years) to be 104cm in length, with a weight of 17kg

4.3.1 Methods

The dynamic dose prediction model was used to run a series of simulation tests for the paediatric settings on the Lodox Statscan. The baseline measurement was the dose predicted with no added filtration, a normal paediatric full-body scan.

Several scans were simulated for each filter material selected, with only the thickness of the filter material being altered between simulations. Filters were then applied to obtain images which were used in a preliminary study to assess image quality. The literature review highlighted the filtration methods and materials which have successfully been used for filtration of X-ray beams. Some materials are better suited to industrial filtration needs, where the tube voltages are much higher than those necessary for medical imaging.

This study examined the filter materials which the literature referred to as preferable for low tube voltage medical imaging such as: copper (Hansson et al. 1997; Brosi et al. 2011), aluminium (Mooney & Thomas 1998), tungsten (Regano & Sutton 1992) and molybdenum (Martin et al. 1999).

4.3.2 Results

Entrance Dose Prediction

Table 3 shows the simulated entrance dose measurements for filtration with aluminium, copper, molybdenum and tungsten at varying thicknesses as predicted by the model. The percentage entrance dose reduction from the standard energy beam spectrum is also displayed.

Table 3: Doses predicted by the dynamic dose prediction model for added filtration

Filter Thickness [mm]	Predicted Dose [µGy]	Dose Reduction [%]
No Filter Material		
0	64.73	0%
Aluminium Filter		
1	50.32	22%
2	40.55	37%
3	33.48	48%
4	28.13	57%
Copper Filter		
0.1	40.87	54%
0.2	25.61	71%
0.3	18.02	80%
0.4	13.5	85%
0.5	10.51	88%
Molybdenum Filter		
0.1	18.7	79%
0.2	8.4	90%
0.3	4.64	95%
0.4	2.83	97%
Tungsten Filter		
0.1	10.11	89%
0.2	3.04	97%
0.3	1.03	99%

The graph displayed in Figure 27 provides a visual summary of the predicted entrance dose reduction for all four materials relative to the increase in filter material thickness. The lower percentage dose reduction shows that the aluminium has a less harsh hardening effect on the output dose when compared to the other materials. The other materials removed well over 50% of the radiation. The amount of photons transferred for accurate imaging is related to the amount of radiation to which the patient is exposed. The 0.1mm copper filter was the only other filter material and thickness to produce a predicted dose higher than 40µGy, with a dose reduction of 50%. All other simulated predicted doses were less than 25µGy and removed the majority of

the incident radiation, and would thus have a significant impact on the image quality if used as a filter material.

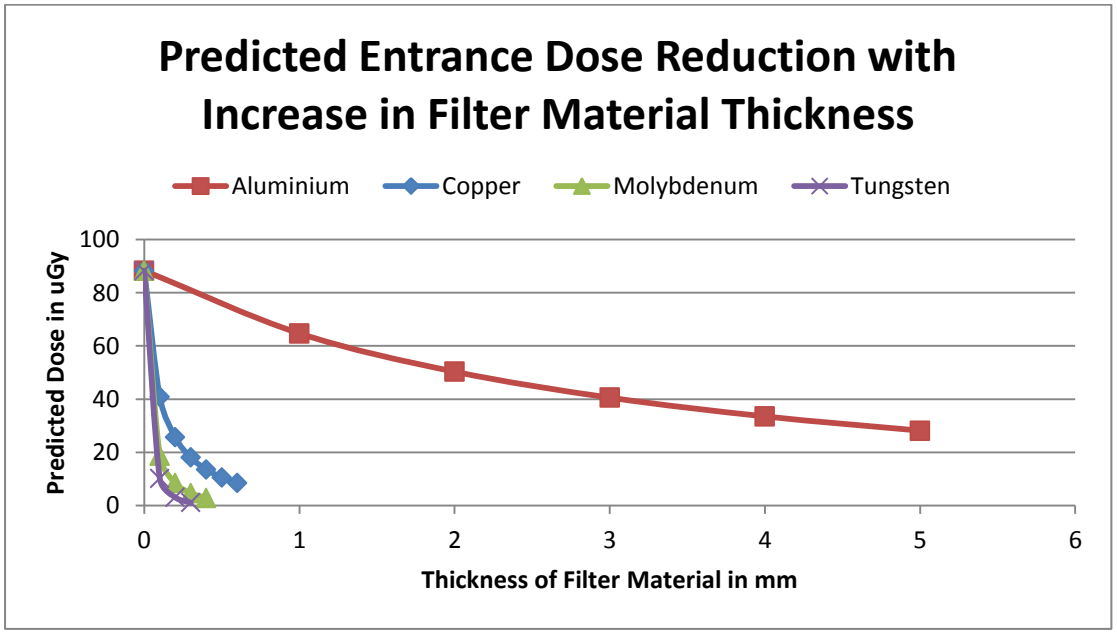

Figure 27: Estimated entrance dose reduction relative to an increase in filter material thickness.

Image Quality Assessment

Image quality was assessed visually to determine whether images would be diagnostically useful after filtration. For all images examined where an entrance dose was lower than 30µGy the image quality was compromised as not enough photons were available to provide adequate imaging. Below in Figure 28 is an example of such an image showing poor contrast quality, where the small discs are not visible, and the large discs are barely visible.

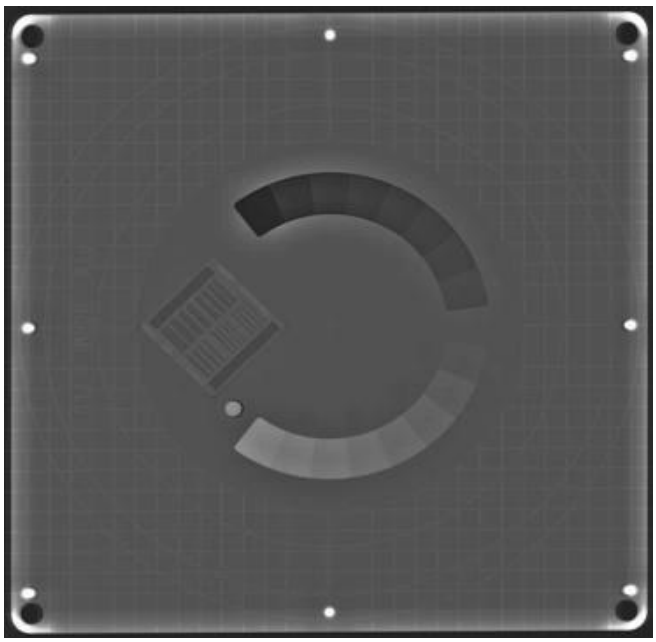

Figure 28: Example of the PTW phantom where the beam has been over-attenuated and the image contrast is poor.

Molybdenum and tungsten both proved to attenuate the generated beam heavily. Molybdenum has proved to be successful filtration materials for mammographic imaging, where the tube voltages are very low (10-35kV)

compared to general X-ray imaging. The Lodox Statscan paediatric settings for tube voltage are significantly higher, at 80kV. The dynamic dose prediction model showed that at 0.1mm tungsten and molybdenum would not be effective, due to the majority of the incident radiation being removed (most cases over 80% removed). At lesser thicknesses than those examined in the model, these materials would become brittle and difficult to manage. This would make the use of molybdenum or tungsten as a paediatric filter material impractical. Thus, these materials eliminated them from the study as potential filter materials.

The dynamic model suggested that a copper filter of thickness 0.1mm was potentially suitable. Aluminium proved to be another suitable theoretical filter, with the varying filter thickness providing a more subtle gradient of beam hardening – thus allowing a greater range of thicknesses to be examined. Added aluminium filter thicknesses of in the range between 1mm and 3mm were found to be potentially suitable for a new paediatric filtration technique as thicknesses greater than this reduced the predicted dose by more than 60%, which would eliminate a significant amount of photons and negatively affect image quality.

4.4 Conclusion

Following the successful development of a static dose prediction model by Irving (2008), a dynamic dose prediction model has been developed to improve the usability of the already validated model.

The dynamic model provides a graphic user interface that is easy-to-use, and displays the predicted beam spectra, organ doses, entrance and effective doses for a broad range of variable inputs.

The dynamic dose prediction model was used to compare the theoretical effectiveness of a variety of filter materials for the standard paediatric scan settings of the Statscan. Aluminium, copper, molybdenum and tungsten were compared, with 2mm and 3mm aluminium filtration and 0.1mm copper filtration being found to be suitable theoretically as acceptable filter materials. The other materials and thicknesses provided too much attenuation to the beam for effective imaging. The dynamic dose prediction model suggests that aluminium and copper could be effective filter materials for developing a new filtration technique for the paediatric settings of the Lodox Statscan.

Studies examined in the literature review promote filtration as an effective dose-reducing technique for paediatric imaging (Brosi et al., 2011; Hansson et al., 1997; Mooney & Thomas, 1998). Brosi et al. found that copper filtration decreased the entrance-surface-dose for paediatric digital X-ray images without consistent decline in image quality, while Mooney and Thomas (1998) found that 3mm aluminium filtration reduced dose with diagnostic image quality maintained. The same study revealed that the attenuation provided by a 3mm aluminium filter to a 55 kV X-ray spectrum was equivalent to that provided by a 0.1mm copper filter.

The next chapter will discuss the development, testing and validation of a new filtration technique for the paediatric settings of the Lodox Statscan.

5. Paediatric Phantom Dose Reduction and Image Quality Study

5.1 Introduction

The previous chapter suggests that aluminium and copper could be effective filter materials for developing a new filtration technique for the paediatric settings of the Lodox Statscan. The purpose of this chapter is to explore these materials in order to find a suitable filtration technique for the Lodox Statscan paediatric settings in order to reduce the ionising radiation dose to the patient, while maintaining diagnostic image quality.

5.2 Methods

5.2.1 Filter Material Selection

Both copper and aluminium are available locally, and are affordable relative to the other materials considered in the model. Both materials are structurally solid at the required thicknesses. Thus the theoretical suitability, affordability, practicality and availability of copper and aluminium made them the preferred filter materials to be used in designing the new filtration technique.

As discussed in 4.4, the dynamic dose prediction model suggested, and the literature confirms, that a filter of 0.1mm copper might be appropriate for the proposed paediatric settings. Similarly, 2mm and 3mm aluminium were also predicted to be advantageous in hardening the X-ray beam enough to reduce dose significantly whilst maintaining image quality. Aluminium filters with a thickness of up to 3.7mm have successfully been used to reduce dose without affecting image quality(Regano & Sutton 1992; Koedooder & Venema 1986).

The filter material needed to be sized in a strip 250mm long and 30mm wide, in order to be placed over the collimator slit, thus providing attenuation to the entire incident beam. A 0.1mm copper strip was cut to size from a large 0.1mm thick sheet of copper. Aluminium sheeting locally available advertised at 1mm in thickness was measured to have a thickness of 0.9mm with Vernier callipers. These aluminium strips could be layered to provide the desired thickness for each set of testing required (eg. 1.8 instead of 2mm, 2.7 instead of 3mm). The dose prediction model was applied to these revised thicknesses for comparison of predicted and measured dose.

The effect that 0.1mm copper filtration has on the image quality for the Lodox Statscan was assessed in Chapter 3 for high tube voltage examinations on the Statscan. As described previously, the use of a 0.1mm copper filter is standard on all Lodox Statscan examinations requiring a tube voltage over 110kV.

Dose Measurement

The PTW UNIDOS dosimeter was used for the dose measurements, as described in 3.2.

5.2.2 Image Quality Assessment

Image quality is the major trade off when lowering radiation (Slovis, 2002). The Normi 4 FLU^{PLUS} test object was selected for comparative assessment of the chosen filter materials and without any added filtration. Changes in contrast and spatial resolution were recorded using the Normi 4 FLU^{PLUS} test object, which gives a numerical value to the contrast and spatial resolution, which was used to assess whether the filter affected the image quality. The spatial resolution (line pairs) and contrast (blocks, large discs, and small discs) were reviewed and recorded. The scoring method is described in the literature review (2.6.3).

An image quality test with the 0.1mm copper filtration was used to assess the effect the filtration would have paediatric Lodox Statscan settings, which use a much lower kV range. The purpose of this assessment was to determine whether the filter, which is already standard on the Statscan, could be applied to the entire range of examinations available.

Baseline Image

The test object was placed on the scan table and imaged using standard Statscan settings. This image was used as a reference or baseline image. The images recorded with the added filtration were then visually compared to the baseline image.

Filtered Image

The test object was scanned with filters applied to the Statscan over the collimator slit, allowing for the incident X-ray beam from the tube to be attenuated by the filter material.

The images were assessed visually by the author and an experienced clinical radiographer. The two observers viewed the images together and conferred over each image assessed.

5.3 Results: 0.1mm Copper Filtration

PTW Normi 4FLU^{PLUS} Phantom for paediatric settings

Figure 29 shows a standard phantom image with paediatric settings, without filtration. The yellow arrows indicate the last two of the five visible larger contrast discs. Figure 30 shows the same object scanned with an added 0.1mm copper filtration. The resulting image showed a significant degradation to the contrast of the test object under diagnostic viewing conditions, with the two discs highlighted by the arrows no longer clearly visible (it should be noted that viewing quality conditions on the diagnostic monitors differs significantly from that of a regular computer monitor or printed paper). Table 4 shows the data obtained from the phantom images. It can be concluded that for the paediatric settings on the Statscan, the 0.1mm copper filter attenuated the X-ray beam beyond the threshold of maintaining image quality.

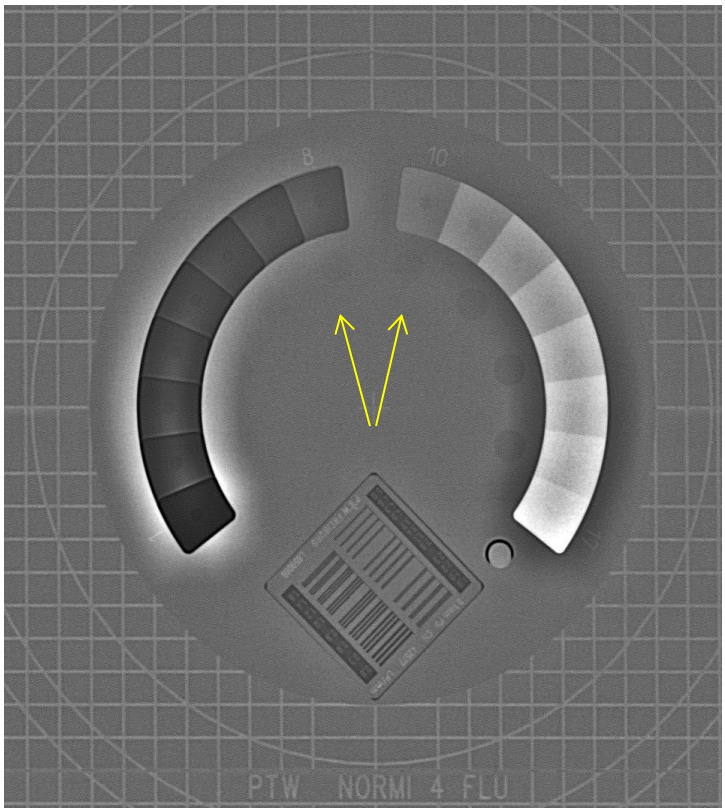

Figure 29: Paediatric full body scan settings, unfiltered, 5 large discs visible.

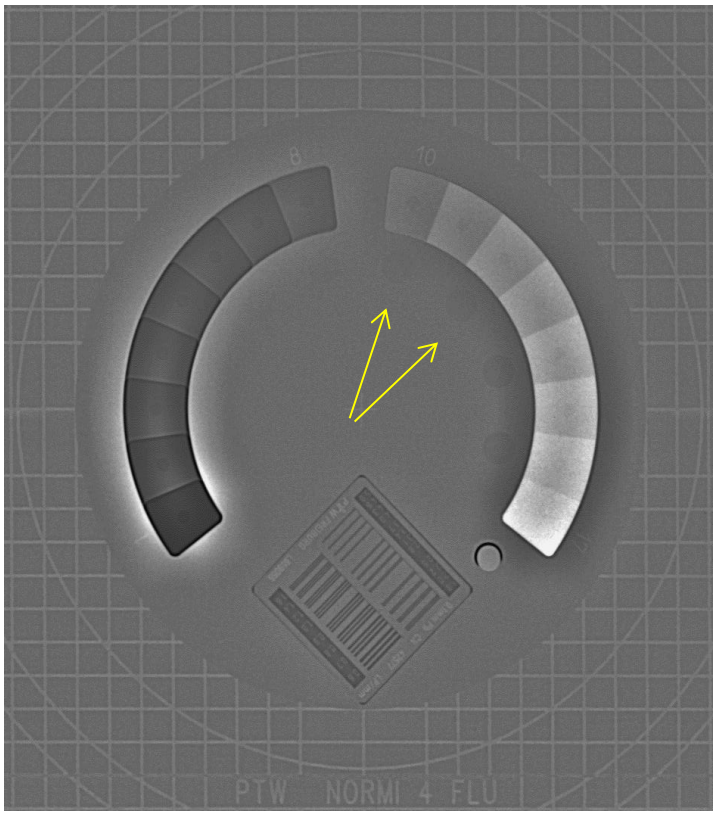

Figure 30: Paediatric full body scan settings, with 0.1mm Cu filtration, 4 large discs visible.

Table 4: Image quality for paediatric settings (80kV, 160mA) with and without 0.1mm copper filtration.

Filter	Phantom Image Quality			
	Line Pairs	Contrast		
		Block	Large Disc	Small Disc
Unfiltered	2.0	17	5	15
0.1mm Cu	2.0	17	4	12

Since image quality was compromised, no dose analysis was performed.

5.4 Results: Aluminium Filtration

A 2.7mm filter of aluminium resulted in visible reduction in contrast when compared to the unfiltered image and the image with 1.8mm aluminium filtration. The visible contrast was scored 17-4-12 for the 2.7mm aluminium filter, compared to 17-5-15 for the 1.8mm aluminium – see Table 5. The examination with 0.1mm copper filtration showed the same contrast levels to that of the 2.7mm aluminium filtration. This confirms the suggestion of Mooney and Thomas (1998) that 3mm aluminium has similar attenuation properties to 0.1mm copper.

The 2.7mm aluminium filter on the paediatric setting did not pass the image quality assessment due to a visible degradation in image quality; Figure 32 shows only four large contrast discs are visible The 2.7mm aluminium filter was thus not considered further. The 1.8mm aluminium filer had no effect on image quality, as shown in Table 5.

Table 5: Image quality for paediatric settings (80kV, 160mA) with and without aluminium filtration.

Filter	Phantom Image Quality without Filter			
	Line Pairs	Contrast		
		Block	Large Disc	Small Disc
No Filter	2.0	17	5	15
1.8mm Al	2.0	17	5	15
2.7mm Al	2.0	17	4	12

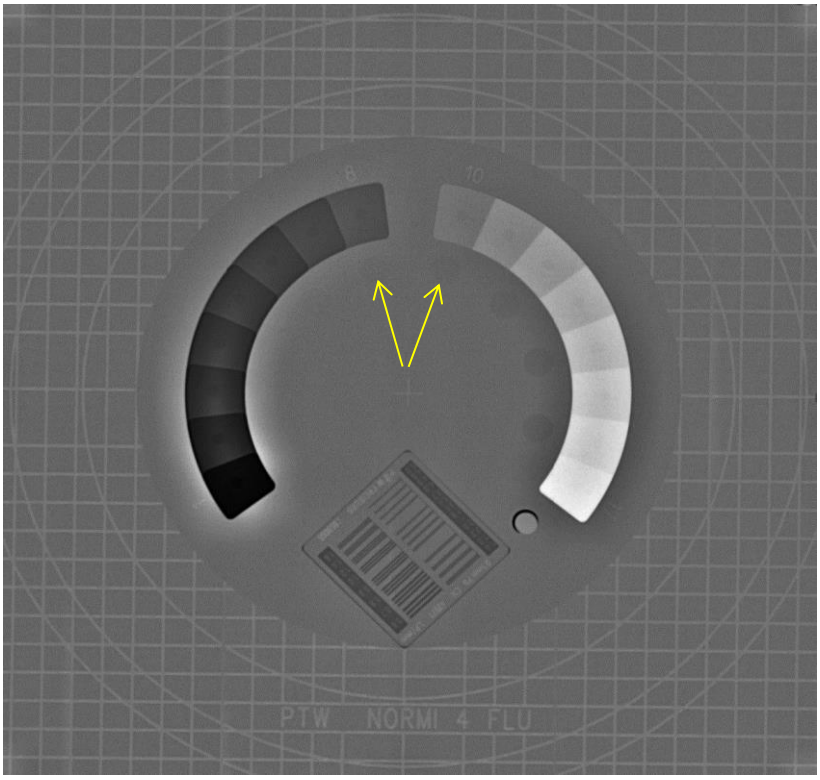

Figure 31: Paediatric full body scan settings, 1.8mm Al filtration, 5 large discs visible.

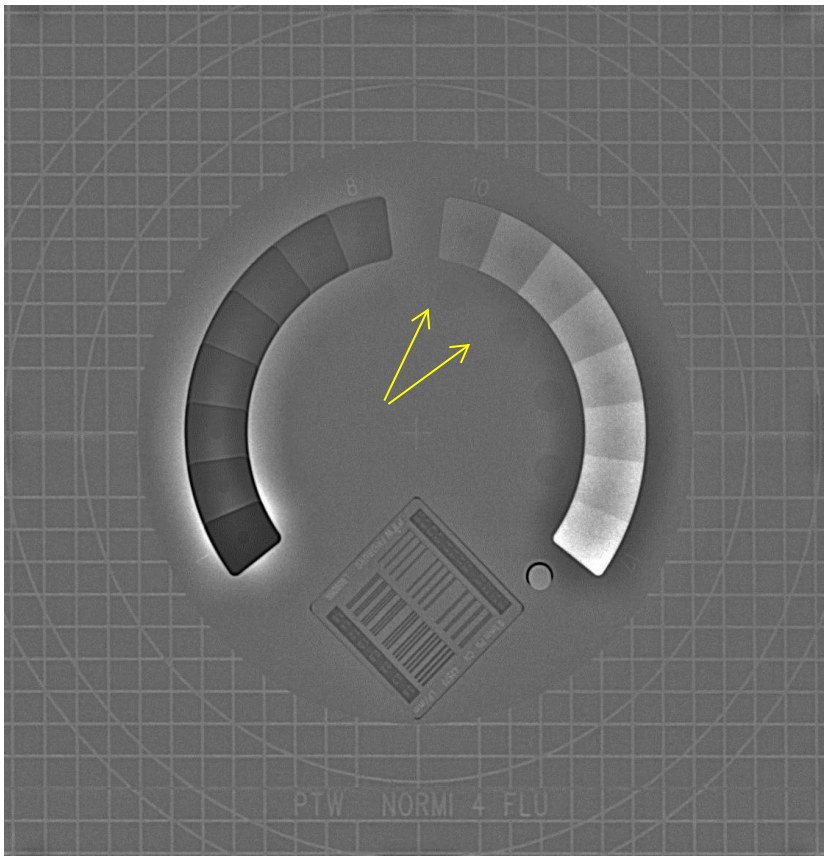

Figure 32: Paediatric full body scan settings, 2.7mm Al filtration, 4 large discs visible.

Table 6 displays the data recorded with the PTW dosimeter for varying aluminium filtration thicknesses for standard AP paediatric settings for the Statscan alongside the predicted doses expected from the dynamic dose prediction model. The 2.7mm aluminium filter was not tested due to its degradation of image quality during the testing described above. The dose measurement with an added 1.8mm aluminium filter showed a dose reduction of 35.8%. The predicted doses were within 6.5% of the measured doses.

Table 6: Examination of dose with aluminium filtration for the standard AP Full Body settings .

Statscan Setting	Filtration	Predicted Dose (µGy)	Corrected Dose	Dose reduction with filter (%)
Paediatric	No Filter	64.73	60.76	-
	1.8mm Al	41.04	39.01	35.8%
	2.7mm Al	34.22	N/A	N/A

5.5 Conclusion

In this chapter, both copper and aluminium were assessed for their viability as a filter material for the paediatric settings of the Lodox Statscan.

The study found that copper was not a suitable attenuation material for paediatric scanning on the Lodox Statscan. The 0.1mm copper filter has been validated for high kV studies, but this study found that the low kV energy spectrum associated with paediatric radiology caused a reduction in image quality when the filter was applied. The paediatric studies reviewed in the literature which used copper as a filtration technique could not be directly compared to this study, as (Hansson et al. 1997) used tube voltages higher than 100kV, while (Brosi et al. 2011) did not investigate image quality specifically and focussed on dose reduction.

Aluminium was found to be a useful filter material in that it reduced dose without affecting image quality for all the standard paediatric settings of the Lodox Statscan. The images obtained using 1.8mm aluminium filtration showed identical image quality to the baseline image when using the PTW phantom to assess contrast and limiting spatial resolution (line pairs). The dose reduction available from using the 1.8mm aluminium filtration technique was 35.8% for measured effective dose. An aluminium filter 1.8mm in thickness was selected as the new filtration technique to be used for the paediatric settings on the Statscan in order to significantly reduce dose without negatively affecting the image quality.

A paediatric cadaver study was used to validate the proposed filtration technique in a clinical setting, as described in the following chapter. The aim of this study was to verify the predicted dose reduction and ensure that image quality is maintained, specifically with regard to anatomical features.

6. A Paediatric Cadaver Study using Aluminium Filtration

6.1 Introduction

The development of a new filtration technique (using 1.8mm aluminium) for Lodox Statscan paediatric imaging and its validation using a phantom has been described in the previous chapters. The next step is to validate the technique in a clinical application. Due to the risks inherent in X-ray radiation, a clinical trial with paediatric patients was not warranted, and a cadaver imaging trial was conducted to verify that image quality is maintained.

6.2 Background

The literature reviewed suggests a need for relevant anatomical background to be in the image for image quality assessment (Sund et al. 2004; Båth 2010). While test objects are useful for objective image analysis, using real human tissue best illustrates the effectiveness of a filter in maintaining image quality for the visualisation of tissues of interest while reducing dose to the patient. Testing the filtration technique on cadaver specimens enables examination of anatomical image quality without harmful radiation exposure to living tissue. An added benefit of using cadavers is that they can be scanned multiple times without any movement, providing ideal conditions for comparing two images with different filtration settings. Ethics approval was necessary before any testing on cadavers could be performed (Båth 2010; Sund et al. 2004; Martin et al. 1999) and was obtained from the Human Research Ethics Committee of the Faculty of Health Sciences.

6.3 Materials & Methodology

6.3.1 X-ray unit

All examinations that form part of this imaging study were performed on the Lodox Statscan digital X-ray system. The tube has an inherent filtration of 1mm Al, while the study examines the effects of an additional 1.8mm Al filter on entrance and effective dose, and image quality.

All examinations were performed using the standard Statscan paediatric settings as shown in Figure 33. The tube configuration for this setting has a voltage of 80kV and a current of 160mA.

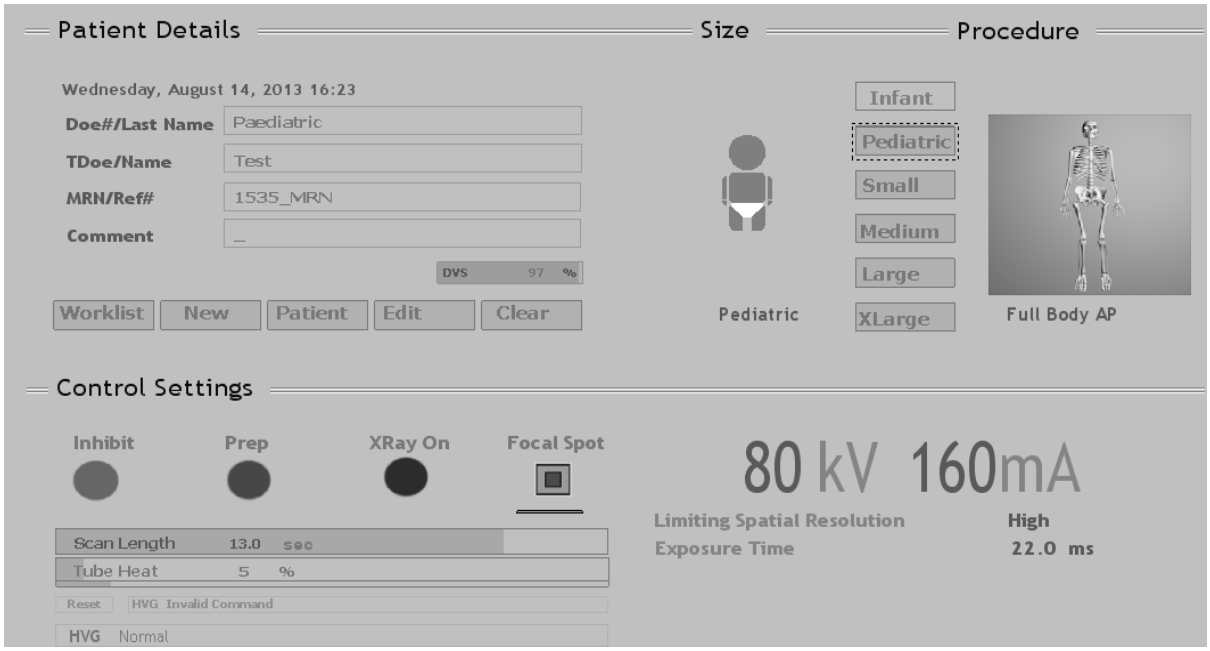

Figure 33: Standard paediatric settings for the Lodox Statscan as shown in the user interface of the Statscan workstation.

6.3.2 Data acquisition

The data for the paediatric cadaver trial was collected from the Salt River Forensic Pathology Laboratory. Over a period of one month, the laboratory was contacted daily to investigate the availability of test subjects. During this study time frame, a total of fourteen test subjects were selected for the imaging study. These were the only available subjects that met the following inclusion criteria:

- Paediatric age, 0-4 years
- No significant disfigurations which may affect assessment of image quality

A code was assigned to each cadaver to provide anonymity. The age, sex, size and weight of each cadaver was recorded.

The steps below describe the procedure for scanning each test subject:

Step 1: Cadaver placement

The table was first moved to the lowest position, thus allowing for the detector to be as close to the cadaver as possible. The cadaver was then placed in a supine position on the table. Due to the small size of some of the cadavers, consistent positioning in the supine position was difficult. Some subjects were clothed, and if buttons/pins were found to affect the image these clothes were removed.

Step 2: Dose measurement

The entrance dose to the test subject was recorded using a PTW UNIDOS dosimeter together with a 30 cc, 300V PTW ionization chamber. The calibration certificate of the PTW dosimeter assures accuracy to within 5% of the measured value. All measurements were taken free-in-air, measured in µGy.

Air temperature and pressure were recorded for each scanning session in order to generate the dose correction factor which needs to be applied to each PTW Unidos dosimeter reading. The PTW 30 cc ionization chamber (type 23361) was placed between the test subject legs so as not to interfere with the anatomical image (see Figure 34).. The probe was placed level with the chest height to simulate skin-entrance dose at the chest height. This was to record skin entrance dose at chest level, in order to obtain the most accurate entrance dose “free in air”, with the smallest amount of backscatter and without creating a large artefact over

the chest region. The probe was also measured to be at least 15 cm above the scanner's detector in order to avoid significant backscatter. The dosimeter was set to record dose in μGy for the period of each scan.

To evaluate the effect that the aluminium filtration would have in a clinical setting, the effective doses were calculated from the recorded entrance doses. The size and weight dimensions of each subject scanned were recorded. The computer based Monte Carlo program, PCXMC Version 2.0, was used to calculate the respective effective dose for each test subject relative to its size and weight dimensions.

The PCXMC software was used to create a theoretical phantom for each test subject. The effective doses were calculated in 29 organs and tissues, and the Monte Carlo program then calculated the total effective dose to the test subject. The current standard tissue weighting factors of the International Commission for Radiological Protection (ICRP) publication 103 (2007) was used in the code (ICRP 2007)..

Step 3: Filtration

Each cadaver was scanned twice, once with the regular paediatric settings, and once with the addition of the additional filtration. For the added filtration scans, a 1.8mm thick strip of aluminium was secured over the collimator slit.

Step 4: Scanning

The scan area selection tool on the imaging workstation was used to define the area of the table which would be scanned. The smallest possible area that allowed for the entire cadaver to be scanned was selected to minimize the total output dose from the tube. The code assigned to the cadaver was entered into the patient name area, along with a notation to state whether added filtration was applied to that scan. Simultaneous to the scanning, the dosimeter was manually activated to begin reading the dose for the duration of the scan, and then manually deactivated at the end of the scan. The total dose recorded through the scan period was recorded from the dosimeter on the data sheet with all the subject data. The digital X-ray image was recorded to the database.

Figure 34: Paediatric cadaver scanned with two different settings, image with added filtration on the right.

6.3.3 Evaluation of clinical image quality

A panel of radiologists provided their experienced opinion on the image sets using a scoring system similar to that used in previous clinical studies of digital image quality. These studies are described in the literature review section 2.6.5 (Hamer et al. 2005; Hansson et al. 1997). These scoring systems are modified from the European Guidelines on Quality Criteria for Diagnostic Radiographic Images.

The panel comprised three experienced radiologists, two of whom had five years' experience, while the third had seven years' experience in medical imaging diagnosis. All three radiologists had specific experience with paediatric radiology.

Each radiologist was presented with pairs of standard DICOM images to examine. Each paired image set provided the reviewer with an identical target subject, imaged under two different filtration settings. The radiologist was blinded as to which image was the control, and which image had added filtration. Viewing both images simultaneously on a diagnostic quality split-screen, the two images were compared and scored on the sheet shown in Table 7 under the following five variables:

- Initial impression
- Contrast
- Clarity
- Overall end impression - At this point the radiologists were allowed to alter the window and level settings of their screens when viewing the images. This is an important step in taking advantage of the image manipulation tools available to radiologists with digital imaging. The radiologists optimised each image and then scored them.
- Whether the images were of diagnostic quality, with or without image manipulation.

The five variables described above were scored subjectively by the reviewing radiologist using a five point scoring scale:

1 – *Much worse, distinct negative differences when compared to the other image*
2 – *Slightly worse, slight negative differences were noticeable when compared to the other image*
3 – *Equivalent, the images were of similar standard and no differences were noted*
4 – *Slightly better, slight positive differences were noticeable when compared to the other image*
5 – *Much better, distinct positive differences when compared to the other image*

Table 7: Relative scoring of the filtered image and the standard image; radiologists were blinded as to which was filtered.

Full Body AP	Much Worse	Slightly Worse	Equivalent	Slightly Better	Much Better
Initial					
Contrast					
Clarity					
Overall					
Diagnostic Quality, Image 1				YES or NO	
Diagnostic Quality, Image 2				YES or NO	

6.3.4 Statistical analysis

The data recorded during the cadaver study were analysed statistically, and comparisons were made for the paired samples, both for the dose reduction and the image quality data sets.

Entrance and Effective Dose Reduction

The entrance dose was measured in µGy. The entrance dose was then "corrected" for environmental factors at the time of recording, such as air temperature and pressure. The corrected dose was for all analysis and comparisons.

The effective dose recordings are the PCXMC doses for the same 14 pairs of scans. These are a computer conversion from entrance dose to effective dose (measured in Sv) based on the patient dimensions. The current standard organ-dose weighting method was used for calculating effective dose, namely ICRP103. Both methods were examined in this study for comparison purposes, thus two sets of paired results are available for effective dose reduction analysis.

The literature suggests that a paired t-test is suitable for assessing dose reduction (Hamer et al. 2005). Both the paired t-test and Shapiro Wilks method were used to assess the data recorded in the dose reduction study.

Clinical Image Quality

12 cadaver image pairs were used for the image quality maintenance study. Two cadavers were rejected from the image quality study, both due to clothing and post-mortem artefacts visible in the image.

With the knowledge that the filtration reduces dose to the test subject, the following definition of a positive result was used: Any image with added 1.8mm aluminium filtration reviewed as "equivalent", "slightly better" or "much better" than the corresponding unfiltered image.

Image quality assessment data provided by three independent radiologists was reviewed and analysed. The "Initial Impression", "Contrast" and "Clarity" factors were reviewed to assess the standard imaging capabilities of the Lodox Statscan paediatric settings without image manipulation. The "End Impression" the "Diagnostic Quality" of the image followed the radiologist taking advantage of the digital image enhancing techniques available to them.

The reviewing radiologist's observations were compared, and their percentage agreement was calculated.

6.4 Results

6.4.1 Entrance dose reduction due to filtration

A total of fourteen paired samples were recorded for the paediatric dose measurement study over a trial period of one month. There were no statistically significant differences in the age, weight or size of the subjects; demographic data are shown below in Table 8. The male-female ratio was even, and all the subjects were within an age spread of 14 days to 1 year.

Table 8: Demographic Data for 14 Paired Cadaver Scans: Dose Recordings

Variable	Value
Sex: Female	7 (50%)
Sex: Male	7 (50%)
Average Age (months)	3.0
Age range	14day – 1year
Weight (kg)	5.0 ± 2.1
Body length (cm)	54.1 ± 8.0

The fourteen subjects were each scanned twice on the Statscan. The scans which contained no added filter material were used as the control set. Table 19 in Appendix A shows these results.

Table 9 provides a statistical summary of the recorded entrance doses. The mean dose for the unfiltered scan dose recordings was calculated to be 72.66µGy ± 2.42µGy. The mean dose for the filtered scan dose recordings was calculated to be 46.53µGy ± 2.18µGy. The mean difference between filtered and unfiltered dose (dose reduction) was 26.48µGy ± 0.72µGy. The standard deviation for all three sets of data was found to be less than 3%. This result shows that the dose recordings for scans with added aluminium filtration were 37% lower on average than in the control group. The recorded data was found to be normally distributed by the Shapiro Wilk's test (p-values>0.05), although the data sample size available was smaller than is usually accepted for this test (see Table 10).

Table 11 shows the Paired T-test results for the entrance dose, where the 95% CI was found to be 71.26 – 74.06 µGy for the unfiltered case, and 44.92 – 47.45 µGy for the filtered case, with a reduction of 26.06 – 26.89 µGy.

Table 9: Statistical summary for cadaver trial entrance dose recordings with and without filtration

Summary Statistics [µGy]					
	Obs	Min	Max	Mean	Std Dev.
No Filter	14	69.11	76.25	72.66	2.42
Filtered 1.8mm Al	14	42.81	49.53	46.19	2.18
Dose Reduction	14	25.29	27.89	26.48	0.72

Table 10: Shapiro Wilks test of Normality for Entrance Dose Reduction

Shapiro Wilks Test of Normality					
	Obs	**W**	**V**	**z**	**Prob>z**
No Filter	14	0.93093	1.278	0.483	0.31439
Filtered 1.8mm Al	14	0.94705	0.98	-0.04	0.51587

Table 11: Paired T-test for Entrance Dose Reduction.

Paired T-test						
	Obs	**Mean**	**Std. Err.**	**Std. Dev.**	**95% Conf Interval**	
No Filter	14	72.66	0.65	2.42	71.26	74.06
Filtered 1.8mm Al	14	46.19	0.58	2.18	44.92	47.45
Dose Reduction [µGy]	14	26.48	0.19	0.72	26.06	26.89

6.4.2 Effective dose reduction due to filtration

Table 21 in Appendix A displays the demographic data for each cadaver which was used in the dose reduction study. The body length and weight was used in the PCXMC Monte Carlo simulator to create a phantom. The effective dose to subject was then calculated within the program using the recorded skin entrance dose and the custom generated phantom for each subject.

The generated effective doses are recorded in Table 19 in Appendix A. For the range of doses examined, the results were fairly similar when comparing the two sets of weighting factors. The average dose reduction achieved with the aluminium filter was found to be 27%.

Table 12 provides a statistical summary of the recorded effective doses. The effective mean dose for the unfiltered scan recordings was calculated to be 0.061mSv ± 0.003mSv. The mean effective dose for the filtered scan was calculated to be 0.044mSv ± 0.003mSv. The mean effective dose reduction for the filtered scan was calculated to be 0.016mSv ± 0.001mSv. This shows an average dose reduction of 27% for the subjects scanned with the added aluminium filtration. The standard deviation for all data was found to be less than 5%.

The recorded data was found to be normally distributed by the Shapiro Wilk's test (p-values>0.05), although as mentioned before, the data sample size available was smaller than is usually accepted for this test (see

Table 13). Table 14 shows the Paired T-test results for the ICRP103 effective doses, where the 95% CI was found to be 0.059–0.063mSv for the unfiltered case, and 0.043–0.046mSv for the filtered case, with a reduction of 0.016–0.017mSv.

Table 12: Statistical summary for cadaver trial effective dose calculated readings with and without filtration

Summary Statistics [mSv]					
	N	**Min**	**Max**	**Mean**	**Std Dev.**
Unfiltered	14	0.055	0.066	0.061	0.003
Filtered	14	0.039	0.049	0.044	0.003
Dose Reduction	14	0.014	0.019	0.016	0.001

Table 13: Shapiro Wilks test of Normality

Shapiro Wilks test of Normality					
	Obs	**W**	**V**	**z**	**Prob>z**
Unfiltered	14	0.95517	0.83	-0.368	0.6434
Filtered	14	0.9758	0.448	-1.581	0.94308

Table 14: Paired t-test results for the effective dose recordings.

Paired T-test						
	Obs	**Mean**	**Std. Err.**	**Std. Dev.**	**95% Conf. Interval**	
Unfiltered	14	0.061	0.001	0.003	0.059	0.063
Filtered	14	0.044	0.001	0.003	0.043	0.046
Difference	14	0.016	0.000	0.001	0.016	0.017

6.5 Image quality assessment

A total of twelve paired samples were examined for image quality over a trial period of one month, as two of the original 14 subjects were found to have artefacts affecting image quality when scanned. There were no statistically significant differences in the age, weight or size of the subjects. The demographic data are shown below in Table 15.

Table 15: Demographic Data for 12 Paired Cadaver Scans: Image Quality Assessment.

Variable	Value
Sex: Female	7 (58%)
Sex: Male	5 (42%)
Age (months)	3.3 ± 3.1
Weight (kg)	5.2 ± 2.1
Body length (cm)	54.2 ± 8.6

Figure 35 and Figure 36 on the next page show examples of the images assessed by the reviewing radiologists on a split-screen monitor. The Window Level bar seen on the right side of the screen was used to enhance the image viewing conditions to suit the radiologist.

Table 16 provides a summary of radiologist's observations when asked to compare the twelve image sets of the cadavers with the filtration technique applied and with the control image (unfiltered). The radiologists were blinded as to which of the two images had added filtration. The desired result was for the filtered image to be considered to have equivalent or image quality.

The opinion of the three radiologists was that the image quality for the paediatric cadaver trial images was equivalent or better with the added filtration in the majority of cases. The radiologists found that for "initial impression" the filtered image was equivalent or better for 89% of the image sets, on average across the three observers. Similarly, the "contrast" assessment had an average score of 83% equivalent or better and the "image sharpness" had an average score of 75% equivalent or better.

The radiologists were then allowed to manipulate the images with their image viewing software as they would in regular practice. The "end impression" showed a 92% agreement between the radiologists, on average, in favour of equivalent or better image quality with filtration, while there was 100% agreement between them that all the filtered and unfiltered images were of clinical diagnostic quality. This indicated that even though the image sets were not all equivalent, they were still found to be of diagnostic quality.

Table 16: Radiologists' perceptions: percentage of filtered images considered to be equivalent and/or better than the unfiltered image.

Category	Radiologist 1	Radiologist 2	Radiologist 3	Average
Initial Impression	67%	100%	100%	89%
Contrast Assessment	58%	92%	100%	83%
Image Sharpness	50%	75%	100%	75%
End Impression	83%	92%	100%	92%
Diagnostic Quality YES	100%	100%	100%	100%

Figure 35: Left image (TIM007A) has no filtration, right image (TIM007B) has 1.8mm Al filtration

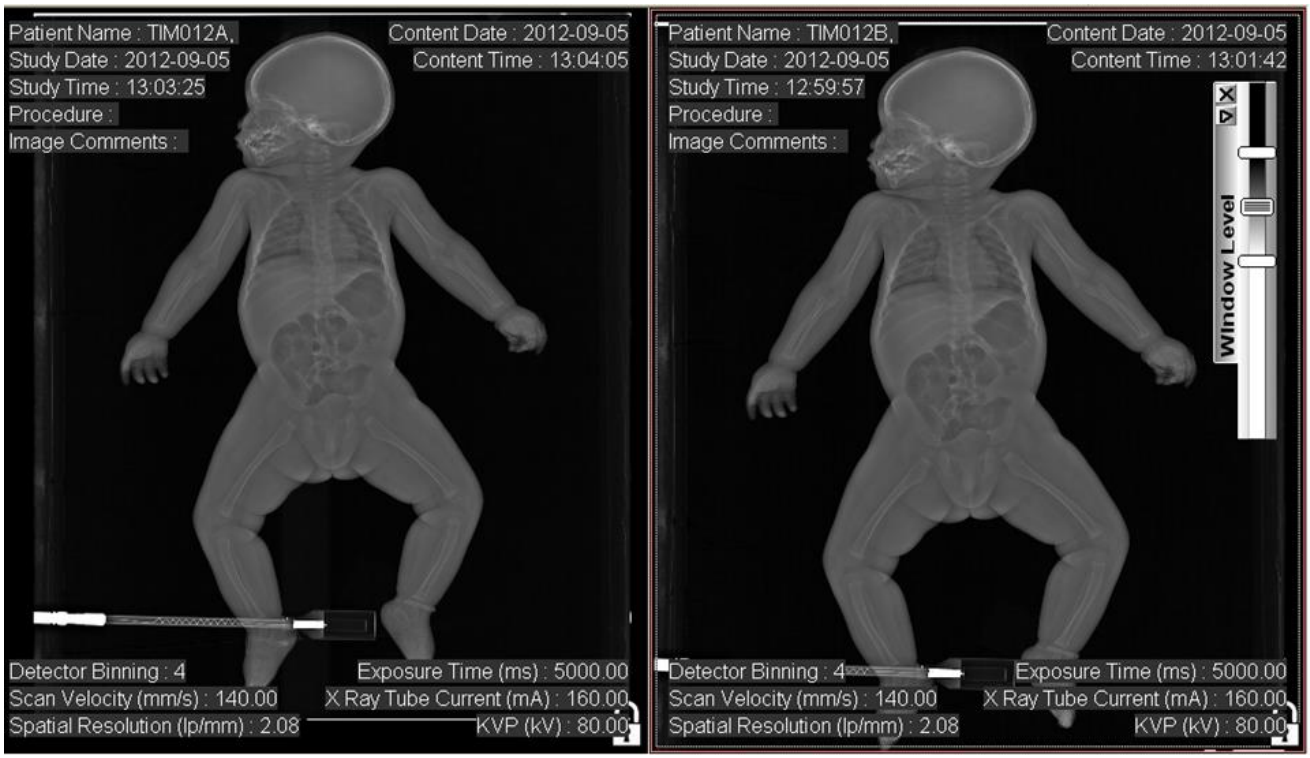

Figure 36: Left image (TIM012A) has 1.8mm AL added filtration, right image (TIM012B) has no added filtration

Discussion

The paediatric cadaver study successfully applied a new filtration technique to the paediatric settings of the Lodox Statscan at the Salt River Forensic Pathology Laboratory. The proposed filtration technique was an added 1.8mm aluminium filter placed over the collimator slit of the Statscan.

The dose reducing ability of the filtration technique was found to be high, as it lowered the average entrance dose by 37%. The average effective dose to the test subject was found for be lowered by 27% on average using the ICRP103 weighting factors.

The image quality was found to be maintained overall when applying the new filtration technique. Three independent radiologists each reviewed the filtered images to be of diagnostic quality. Assessing image quality is a complex task, and although there was some disagreement, every variable assessed found the filtered image to be equivalent and/or better than the standard image most of the time, and the filtered image was always of diagnostic quality. There was some change in contrast to the filtered image, as is expected with added filtration, but the change in contrast did not negatively affect the clinical image quality.

These results are in line with the finding of (Mooney & Thomas 1998) as described in section 2.5.2. The aluminium filtration reduced entrance dose significantly and reduced effective dose, while image quality was not affected. The result demonstrates that paediatric filtration techniques are possible for the Lodox Statscan, and this new method of reducing dose to paediatric patients can be extended to other LSSR systems.

The image quality analysis method was adapted from that used by (Hamer et al. 2005). Future studies should have all the radiologists reviewing the images on the same viewing station, as separate view stations may have impacted the viewing conditions and each viewing monitor has different contrast settings with can significantly impact the first impression when reviewing an image. Each individual radiologist did, however, review all images on one viewing station, thus the individual comparisons of the two data sets took place under the same viewing conditions. One radiologist, following the same image review method as the other two radiologists, reviewed all the images pairs as equivalent.

7. Conclusion

The Lodox Statscan currently has a 0.1mm copper filter in place for all scans requiring tube voltage over 110kV. The first objective of this study was to show that this filter did not alter image quality when applied, thus proving the concept of filtration as effective for linear slot scanning radiography.

Prior to this study, a static dose prediction model had been developed for the Lodox Statscan. This model was adapted to become more dynamic, allowing for the variation of input technique factors. More specifically, the new graphic user interface allowed for the input variables to be easily manipulated, while the output data and graphs changed automatically on the screen in real time. One major addition to the model was the ability to change the type of filter material, and the thickness of the filter. These changes allow the dynamic dose prediction model to become an effective tool in assisting the selection of filter materials for proposed filtration techniques.

The dynamic dose prediction model was used to develop a paediatric filtration technique that could be used on all the standard paediatric settings for the Lodox Statscan. The proposed technique was implemented, and a series of phantom tests showed that adding 1.8mm aluminium to the Statscan as an additional filter reduced entrance dose significantly without affecting image quality.

The new filtration technique of applying a 1.8mm added aluminium filtration to the standard paediatric scan settings was tested in a clinical environment involving paediatric cadavers as the test objects. Experienced radiologists assessed the filtration technique positively, describing that in all cases the image quality was equivalent or better with the added filtration. All the images from the cadaver study were found to be of diagnostic quality. The dose reduction in the cadaver study was substantial, with the average entrance dose being 37% less with the added filtration. The average effective dose was calculated to be lower also, by 27% on average.

This is the first instance of a paediatric specific filtration technique being applied to the Statscan, and the successful validation of this technique brings the future possibility of individual filtration techniques for each of the standard settings on the Statscan.

Thus the primary objective of this thesis was achieved, with the development and validation of a new paediatric filtration technique for the Lodox Statscan, which reduces dose significantly while maintaining diagnostic image quality.

Future work could include the addition of detector quantum efficiency (DQE) as an added image quality measure of detector performance now that a method for clinical image quality has been established and verified. There is much room for further optimisation of filtration techniques for the Lodox Statscan throughout all the standard settings. The filtration techniques for very high kV (extra-large patients) settings and low kV (paediatric patients) settings have validated, but filtration techniques have not been examined for the small, medium and large sized patients. Further optimisation could see all the standard settings on the Statscan having a particular filtration technique to reduce dose whilst maintaining image quality.

A mechanical design project should be undertaken to investigate methods of inserting different filtration materials into the path of the incident beam. This would enable the Statscan to apply different filters depending on the scan selected.

8.References

Båth, M., 2010. Evaluating imaging systems: practical applications. *Radiation Protection Dosimetry*, 139(1-3), pp.26–36.

Behrman, R.H. & Yasuda, G., 1998. Effective dose in diagnostic radiology as a function of x-ray beam filtration for a constant exit dose and constant film density. *Medical physics*, 25(5), pp.780–90.

Beutel, J. et al., 2000. *Handbook of Medical Imaging: Physics and Psychophysics*, Washington: Society of Photo-Optical Instrumentation Engineers.

Boone, J.M., 1992. Paramtrized x-ray absorption in diagnostic radiology from monte Carlo calculations: Implications for x-ray detector design. *Medical physics*, 19, pp.1467–1473.

Boone, J.M. & Seibert, J.A., 1997. An accurate method for computer-generating tungsten anode x-ray spectra from 30 to 140 kV. *Medical Physics*, 24(11), pp.1661–1670.

Brosi, P. et al., 2011. Copper filtration in pediatric digital X-ray imaging: its impact on image quality and dose. *Radiological physics and technology*, 4(2), pp.148–55.

Busch, H.P. & Faulkner, K., 2005. Image quality and dose management in digital radiography: a new paradigm for optimisation. *Radiation protection dosimetry*, 117(1-3), pp.143–7. Available at: http://www.ncbi.nlm.nih.gov/pubmed/16461521 [Accessed September 8, 2011].

Dobbins, J.T., 2000. *Handbook of Medical Imaging: Physics and Psychophysics, Volume 2*,

Douglas, T. et al., 2008. Early detection of fractures with low-dose digital X-ray images in a pediatric trauma unit. *The Journal of trauma*, 65(1), pp.E4–7. Available at: http://www.ncbi.nlm.nih.gov/pubmed/17514040 [Accessed September 20, 2011].

Doyle, C.A. & Brennan, P.C., 1999. Technical note Erbium filtration : a cost-effective , dose-reducing filter which maintains abdominal image quality. *European Radiology*, 1925, pp.1923–1925.

Esterhuizen, W., 2010. *The Effects on Image Quality with 0.2mm and 0.6mm of Copper Filtration on the Incident X-ray beam*,

Evangelopoulos, D.S. et al., 2010. Impact of Lodox Statscan on radiation dose and screening time in paediatric trauma patients. *European Journal of Pediatric Surgery*, 20(6), pp.382–6.

Exadaktylos, a K. et al., 2008. Total-body digital X-ray in trauma. An experience report on the first operational full body scanner in Europe and its possible role in ATLS. *Injury*, 39(5), pp.525–9. Available at: http://www.ncbi.nlm.nih.gov/pubmed/18321506 [Accessed September 20, 2011].

Francke, T. et al., 2001. Dose reduction in medical X-ray imaging using noise free photon counting. *Nuclear Instruments and Methods in Physics Research*, 471, pp.85–87.

Gislason, A.J., Davies, A.G. & Cowen, A.R., 2010. Dose optimization in pediatric cardiac x-ray imaging. *Medical Physics*, 37(10), p.5258.

Gogos, K.A. et al., 2003. Radiation dose considerations in common paediatric X-ray examinations. *Pediatric Radiology*, 33(4), pp.236–40.

Hamer, O.W. et al., 2005. Radiology Chest Radiography with a Flat-Panel Detector : Image Quality with Dose Reduction after Copper Filtration. *Radiology*, 237, pp.691–700.

Hansson, B. et al., 1997. Pediatric radiology Original article Added copper filtration in digital paediatric double-contrast colon examinations : effects on radiation dose and image quality. *The Organ*, 1122, pp.1117–1122.

ICRP, 2007. *The 2007 Recommendations of the International Commission on Radiological Protection*,

Irving, 2008. *Radiation Dose Measurement and Prediction for Linear Slit Scanning Radiography*. University of Cape Town.

Irving, B. et al., 2008. Radiation dose from a linear slit scanning X-ray machine with full-body imaging capabilities. *Radiation protection dosimetry*, 130(4), pp.482–9.

Koedooder, K. & Venema, H.W., 1986. Filter materials for dose reduction in screen-film radiography. *Physics in medicine and biology*, 31(6), pp.585–600. Available at: http://www.ncbi.nlm.nih.gov/pubmed/3755830.

Martin, C., 2007. Optimisation in general radiography. *Biomedical imaging and intervention journal*, 3(2), p.e18.

Martin, C., Sharp, P. & Sutton, D., 1999. Measurement of image quality in diagnostic radiology. *Applied radiation and isotopes*, 50(1), pp.1–19.

Mooney, R. & Thomas, P.S., 1998. Dose reduction in a paediatric X-ray department following optimization of radiographic technique. *British Journal of Radiology*, 71(848), pp.852–60.

Nicholson, R., Tuffee, F. & Uthappa, M.C., 2000. Skin sparing in interventional radiology: the effect of copper filtration. *The British journal of radiology*, 73(865), pp.36–42.

NIST, 1996. NIST X-ray Attenuation Databases. *National Institute of Standards and Technology*. Available at: http://www.nist.gov/pml/data/xraycoef/index.cfm.

Regano, L.J. & Sutton, R., 1992. Radiation dose reduction in diagnostic x-ray procedures. *Physics in Medicine and Biology*, 37(9), pp.1773–88.

Ron, E., 2011. Ionizing Radiation and Cancer Risk : Evidence from Epidemiology. *Radiation Research*, 150(5).

Samei, E. et al., 2005. Radiology Comparative Scatter and Dose Performance of Slot-Scan and Full-Field Digital Chest Radiography Systems 1. , pp.6–8.

Scheelke, M., Potgieter, J.H. & Villiers, M. De, 2005. System characterization of the STATSCAN full body slit scanning radiography machine: theory and experiment. *Proceedings of SPIE*, 5745, pp.1179–1190.

Slovis, T.L., 2002. CT and computed radiography: the pictures are great, but is the radiation dose greater than required? *AJR. American journal of roentgenology*, 179(1), pp.39–41. Available at: http://www.ncbi.nlm.nih.gov/pubmed/12076901.

Smans, K. et al., 2010. Cu filtration for dose reduction in neonatal chest imaging. *Radiation protection dosimetry*, 139(1-3), pp.281–6.

Smet, B.S., 2012. Correlation of Contrast-Detail Analysis and Clinical Image Quality Assessment in Chest Radiography. *Radiology*, 262(1).

Sprawls, P., Physical Principles of Medical Imaging Online. Available at: http://www.sprawls.org [Accessed November 15, 2011].

Sund, P. et al., 2004. Comparison of visual grading analysis and determination of detective quantum efficiency for evaluating system performance in digital chest radiography. *European Radiology*, 14(1), pp.48–58. Available at: http://www.ncbi.nlm.nih.gov/pubmed/14564469 [Accessed September 14, 2011].

Szucs-Farkas, Z. & Vock, P., 2009. Image quality of supine chest radiographs: intra-individual comparison of computed radiography and low-dose linear-slit digital radiography. *European radiology*, 19(9), pp.2156–62. Available at: http://www.ncbi.nlm.nih.gov/pubmed/19415292 [Accessed July 26, 2011].

Tapiovaara M, Siiskonen T. PCXMC – A Monte Carlo program for calculating patient doses in medical x-ray examinations (2nd Ed.). STUK-A 231. Helsinki: Säteilyturvakeskus; 2008.

Trauernicht, C. et al., 2012. Dose Reduction and Image Preservation After the Introduction of a 0 . 1 mm Cu Filter into the LODOX Statscan Unit above 110 kVp. In *International Radiation Protection Association International Congress, Glasgow*. Glasgow.

Walker, J., 2000. *Permissible dose: A history of radiation protection in the Twentieth Century*,

Appendix A

Table 17: Comparison of image quality for all standard Lodox Statscan settings with and without 0.1mm Cu filtration

		Filtered				Unfiltered				Deviation			
Size	**Protocol**	**Line Pairs**	**Contrast**			**Line Pairs**	**Contrast**			**Line Pairs**	**Contrast**		
Paediatric	Abdomen	2.0	16	4	10	2.2	16	4	13	0.2	0.0	0.0	3.0
Paediatric	Chest	1.6	12	0	4	1.8	13	0	4	0.2	1.0	0.0	0.0
Paediatric	Full Body	1.8	16	3	11	1.8	16	4	11	0.0	0.0	1.0	0.0
Paediatric	Pelvis	2.0	16	4	11	2.2	16	4	11	0.2	0.0	0.0	0.0
Paediatric	Skull	2.2	16	4	13	2.5	16	5	13	0.3	0.0	1.0	0.0
Small	Abdomen	2.2	16	4	13	2.2	16	4	15	0.0	0.0	0.0	2.0
Small	Chest	2.0	16	3	10	2.2	16	4	11	0.2	0.0	1.0	1.0
Small	Full Body	1.8	16	4	11	1.8	16	5	13	0.0	0.0	1.0	2.0
Small	Pelvis	2.5	16	4	15	2.5	16	5	16	0.0	0.0	1.0	1.0
Small	Skull	2.2	16	4	16	2.5	16	4	16	0.3	0.0	0.0	0.0
Medium	Abdomen	2.8	16	5	16	2.5	16	4	16	-0.3	0.0	-1.0	0.0
Medium	Chest	2.5	16	5	16	2.5	16	5	16	0.0	0.0	0.0	0.0
Medium	Full Body	2.0	16	4	16	2	16	4	16	0.0	0.0	0.0	0.0
Medium	Pelvis	2.5	16	4	16	2.8	16	5	16	0.3	0.0	1.0	0.0
Medium	Skull	2.8	16	4	16	2.8	16	5	16	0.0	0.0	1.0	0.0
Large	Abdomen	2.2	16	5	16	2.2	16	4	16	0.0	0.0	-1.0	0.0
Large	Chest	3.1	16	5	16	2.8	16	5	16	-0.3	0.0	0.0	0.0
Large	Full Body	2.0	16	4	16	2	16	5	16	0.0	0.0	1.0	0.0
Large	Pelvis	2.0	14	4	12	2	13	4	11	0.0	-1.0	0.0	-1.0
Large	Skull	2.8	16	4	16	2.5	16	4	16	-0.3	0.0	0.0	0.0
X-Large	Abdomen	2.2	13	5	11	2.2	13	5	11	0.0	0.0	0.0	0.0
X-Large	Chest	2.2	16	5	15	2.2	16	5	15	0.0	0.0	0.0	0.0
X-Large	Full Body	1.6	16	4	15	1.6	16	4	15	0.0	0.0	0.0	0.0
X-Large	Pelvis	2.2	13	4	11	2.2	13	5	11	0.0	0.0	1.0	0.0
X-Large	Skull	2.8	16	5	16	2.8	16	5	16	0.0	0.0	0.0	0.0

*The data shown in Table 17 is a secondary study completed in 2011, following the methodology laid out in Chapter 3. The discrepancy in results between Table 2 and Table 17 can be attributed to two factors which affect subjective image quality assessments; a. the person reviewing the images has their own subjective perception of contrast and image quality, and b. the viewing monitor on the Lodox Statscan at UCT was changed from a Philips tube-monitor to a Samsung LED monitor which provides differing standards of contrast.

Table 18: Dose recordings for paediatric cadaver trial with and without aluminium filtration. The dose reduction produced by the addition of the 1.8mm aluminium filter is shown as a percentage in the final column.

	No Filter		Aluminium Filter		
Test #:	Recorded Dose [uGy]:	Corrected Dose [uGy]:	Recorded Dose [uGy]:	Corrected Dose [uGy]:	Reduction of Corrected Dose [%]:
1	73.02	71.38	46.73	45.68	36%
2	77.14	75.41	49.7	48.59	36%
3	71.62	70.17	45.14	44.23	37%
4	70.54	69.11	43.69	42.81	38%
5	72.44	70.23	46.35	44.93	36%
6	74.29	73.66	46.16	45.77	38%
7	71.91	71.30	44.05	43.68	39%
8	70.15	69.56	43.87	43.49	37%
9	72.76	72.15	46.44	46.048	36%
10	74.8	74.17	47.68	47.28	36%
11	76.03	75.39	48.89	48.48	36%
12	76.71	75.23	49.72	48.76	35%
13	74.71	73.27	48.24	47.31	35%
14	77.75	76.25	50.5	49.53	35%

Table 19: Calculated effective dose for paediatric cadaver trial with and without aluminium filtration.

Test #	Unfiltered Effective Doses [mSv]		Filtered Effective Doses [mSv]		Dose Reduction	
	ICRP 60	**ICRP 103**	**ICRP 60**	**ICRP 103**	**ICRP 60**	**ICRP 103**
1	0.07	0.07	0.05	0.05	27%	28%
2	0.06	0.06	0.05	0.05	25%	26%
3	0.06	0.06	0.04	0.04	27%	27%
4	0.06	0.06	0.04	0.04	28%	29%
5	0.06	0.06	0.04	0.04	25%	26%
6	0.07	0.06	0.05	0.05	29%	29%
7	0.05	0.06	0.04	0.04	28%	29%
8	0.06	0.06	0.04	0.04	28%	28%
9	0.06	0.06	0.05	0.05	27%	27%
10	0.06	0.06	0.05	0.05	26%	27%
11	0.06	0.06	0.04	0.04	25%	25%
12	0.06	0.06	0.04	0.04	24%	25%
13	0.06	0.06	0.05	0.05	26%	26%
14	0.07	0.06	0.05	0.05	25%	25%
Average	**0.06**	**0.06**	**0.04**	**0.04**	**27%**	**27%**

Table 20: Demographic data from cadavers used to generate effective dose in the PCXMC software.

Test #:	Age:	Length [cm]:	Weight [kg]:
TIM001	2 weeks	50	2.3
TIM002	2 months	57	5.4
TIM003	4 weeks	59[1]	5.6
TIM004	2 months	50	4.0
TIM005	4 months	60	6.6
TIM006	3 weeks	45	2.7
TIM007	4 months	60	7.8
TIM008	4 months	60	4.0
TIM009	3 days	50	3.1
TIM010	4 months	60	5.6
TIM011	6 months	65[1]	8.2
TIM012	1 year	70	8.6
TIM013	3 weeks	44	3.0
TIM014	1 month	43	2.9

[1] Indicates subject length was not available, and an estimated length was used

Table 21: Radiologists score for the 12 sets of filtered images, with the unfiltered image as the reference image for scoring.

	#	Initial Impression	Contrast Assessment	Image Sharpness	End Impression	Diagnostic Quality
Radiologist 1	1	2	2	2	3	Yes
	2	3	2	2	3	Yes
	3	4	2	3	3	Yes
	4	2	4	4	3	Yes
	5	4	4	3	3	Yes
	6	2	2	2	2	Yes
	7	4	3	2	2	Yes
	8	3	4	4	3	Yes
	9	4	4	3	3	Yes
	10	2	2	2	3	Yes
	11	4	3	2	3	Yes
	12	4	4	4	3	Yes
Radiologist 2	1	5	3	3	3	Yes
	2	4	4	2	3	Yes
	3	4	3	2	3	Yes
	4	5	2	2	3	Yes
	5	5	5	3	2	Yes
	6	4	4	3	3	Yes
	7	4	4	3	3	Yes
	8	4	4	4	3	Yes
	9	4	4	4	3	Yes
	10	3	4	3	3	Yes
	11	3	3	3	3	Yes
	12	4	4	4	3	Yes
Radiologist 3	1	3	3	3	3	Yes
	2	3	3	3	3	Yes
	3	3	3	3	3	Yes
	4	3	3	3	3	Yes
	5	3	3	3	3	Yes
	6	3	3	3	3	Yes
	7	3	3	3	3	Yes
	8	3	3	3	3	Yes
	9	3	3	3	3	Yes
	10	3	3	3	3	Yes
	11	3	3	3	3	Yes
	12	3	3	3	3	Yes